Journal of Biomedical Materials Research Part A

WILEY

Society For Biomaterials

RESEARCH ARTICLE OPEN ACCESS

Decellularised Cartilage-Based Hydrogels Functionalised With Chondroitin Sulphate and Quercetin: The Impact on Chondrogenesis

Nuno Da Silva Rosa[1,2,3] | Nuno Neves[1,2,4,5] | Michael Gelinsky[6] | Susana Gomes Santos[1,2,7] | Anne Bernhardt[6] | Mário Adolfo Barbosa[1,2,3]

[1]i3S—Instituto de Inovação e Investigação em Saúde, Universidade do Porto, Porto, Portugal | [2]INEB—Instituto de Engenharia Biomédica, Universidade do Porto, Porto, Portugal | [3]ICBAS—Instituto de Ciências Biomédicas Abel Salazar, Universidade do Porto, Porto, Portugal | [4]Departamento de Ortopedia, Hospital CUF Porto, Porto, Portugal | [5]MEDCIDS—Departamento de Medicina da Comunidade, Informação e Decisão em Saúde, Faculdade de Medicina, Universidade do Porto, Porto, Portugal | [6]Centre for Translational Bone, Joint and Soft Tissue Research, Faculty of Medicine, Technische Universität Dresden, Dresden, Germany | [7]FCUP—Faculdade de Ciências, Universidade do Porto, Porto, Portugal

Correspondence: Mário Adolfo Barbosa (mbarbosa@i3s.up.pt)

Received: 1 May 2025 | **Revised:** 31 August 2025 | **Accepted:** 22 September 2025

Funding: This work was supported by Fundação para a Ciência e a Tecnologia, through the FETBIO project (FCT-2020-PTDC/BTM-MAT/0438/2020) and doctoral grant SFRH/BD/150920/2021.

ABSTRACT

Tissue engineering and regenerative medicine approaches are being actively developed for degenerative disorders, including osteoarthritis (OA). Decellularized matrix (dECM) is a promising biomaterial; however, glycosaminoglycan (GAG) loss during decellularization limits its chondrogenic potential. In this study, we aimed to overcome this by developing a dECM hydrogel originating from cartilage, functionalized with the GAG chondroitin sulphate (CS), to replenish those originally depleted and incorporating quercetin to enhance hydrogel properties and chondrogenesis. An optimized decellularization protocol efficiently removed DNA, but with a significant loss of GAGs (73%). After dECM solubilization, functionalization with CS or aldehyde modified CS (mCS) was performed. CS-functionalized hydrogels maintained low stiffness compared to non-functionalized hydrogel, while 0.2 mg/mL mCS hydrogels exhibited significantly slower gelation kinetics. To aid the hydrogel's chondrogenic ability, a novel approach using quercetin was investigated. Incorporation of 0.3 mg/mL quercetin in 0.4 mg/mL mCS-functionalized hydrogels resulted in increased gel stiffness. The impact on cell viability and chondrogenic differentiation was evaluated. Results showed similar cell viability in dECM and CS-functionalized hydrogels at 1 and 3 days of culture, with no significant changes in gene expression of chondrogenic and hypertrophic genes. In quercetin-containing hydrogels, the viability of human dermal fibroblasts was not significantly different from non-functionalized hydrogels, while human chondrocytes showed a significant upregulation of collagen type II, with 6.6- and 2.2-fold increases for 0.15 and 0.3 mg/mL quercetin, respectively. These results provide an initial proof-of-concept for dECM functionalization strategies that restore lost CS while incorporating quercetin, creating a microenvironment favorable for cartilage repair.

1 | Introduction

The loss of cartilage and the onset of bone growth are notable during osteoarthritis (OA), a degenerative joint disease affecting an estimated 595 million people globally in 2020 [1]. This pathological cartilage remodeling contributes to the disease being both painful and debilitating for the affected individuals [2, 3], having a high impact upon the workforce and healthcare

[Correction added on 28 October 2025, after first online publication: The copyright line was changed.]

systems [1]. Therefore, the development of new therapeutic tools to repair and regenerate cartilage lesions is urgently required.

Physiologically, the cartilage matrix allows the joint to provide movement for the skeletal system with low frictional resistance [4, 5]. Notably, hyaline cartilage, the main cartilage affected by OA, is rich in collagen type II and proteoglycans including aggrecan, a glycosylated protein containing glycosaminoglycan (GAG). These are vital for the hydration of the extracellular matrix (ECM), a feature that is essential for the transmission of mechanical strains during movement [6, 7]. The cartilage degradation, along with its ossification, leads to pain and loss of joint movement [8, 9].

Cartilage is primarily non-innervated and avascular, with the latter being considered as the main contributor towards the lack of physiological regeneration [10, 11]. Cartilage matrix proteins and GAGs are essential for homeostasis, contributing to chondrocyte resistance to hypertrophy [12, 13]. However, as OA progresses, cartilage matrix degradation intensifies, with the disease managing to overcome the tissue's hindrance for vascularization, innervation, and osteogenesis [14]. Together, these can exacerbate the disease, further preventing cartilage repair [14, 15]. Chondrocyte hypertrophy leads to apoptosis and cartilage calcification onset [16]. Cartilage physiological limitations hinder halting pathological OA progression and cartilage regeneration, key to effective treatment [17].

The ubiquitous presence of the GAG, especially chondroitin sulphate (CS), is widespread in tissues and vital in vitro/in vivo, driving interest in this natural polysaccharide for health [18]. In cartilage ECM, it can constitute up to 50% at birth and 15% in adulthood (depending on species, age, and gender) [19, 20]. Notably, the monomer structure contains a sulphate group along with two sugar units: D-glucuronic acid and N-acetylgalactosamine. CS sulphation varies, mainly as 4- or 6-sulphate variants [21, 22]. The sulphate group is the main contributor to the biopolymer's negative charge, enabling interaction with positive substrates and water [23]. If required, CS can be modified to contain aldehyde groups, proving essential for tissue bioadhesiveness or functionalizing biomaterials. This can be achieved via conjugation to an amine (imine bond) or alcohol group (hemiacetal) [24]. Such modifications can alter the biopolymer properties and should be evaluated for bioengineering applications.

Cartilage-mimicking scaffolds have been developed, including solid implants and injectable hydrogels [25, 26]. Both two-dimensional (2D) and three-dimensional (3D) cultures have been used to ascertain the biological impact of these materials, with the latter having proven to be the most effective in mimicking the in vivo 3D environment [27]. In relation to chondrogenic differentiation studies, the utilization of 2D monolayer cultures has proven subpar in stem cell differentiation and chondrocyte activity. The onset of 3D cell culture approaches appears to have provided the necessary biotechnology platform for in vitro experimentation, enabling the development of approaches focusing on novel proof-of-concept treatments for cartilage regeneration [28].

Previous studies, using different tissues, focused on decellularized extracellular matrix (dECM) scaffolds demonstrating their enhanced biochemical interactions, biodegradability, and biocompatibility [29, 30]. Briefly, obtaining dECM requires the removal of cellular content while retaining the original ECM components [31, 32]. Such approaches rely on the use of physical and chemical processes, which often have the drawback of removing/damaging the GAG content, including CS [33, 34]. Furthermore, when producing dECM-based hydrogels, the required acidic solubilization can cause further alterations to these polymers [35]. Previous studies have determined the ability of cartilage-sourced dECM to ensure differentiated stem cells have a chondrogenic phenotype with the expression of several genetic markers. These include the main collagen of hyaline cartilage, collagen type II, along with other markers, namely aggrecan and cartilage oligomeric matrix protein [32]. The latter is a glycoprotein whose role is to aid in the proliferation of chondrocytes and collagen fibrillogenesis [36]. These all work in tandem to ensure a chondrogenic microenvironment while limiting the onset of chondrocyte hypertrophy, a major complication associated with certain hydrogels as observed when using collagen type I hydrogels [37]. Biomaterials from natural sources generally offer higher biocompatibility and biodegradability and lower immunogenicity compared to synthetic biomaterials like polyethylene glycol [38, 39]. Thus, dECM use in clinics is promising due to reduced host rejection [40]. However, the critical role of GAGs in the chondrogenic microenvironment makes restoring their levels vital to improve the efficacy of dECM in cartilage repair [24, 41]. Considering this, functionalization strategies can be applied to reconstitute the GAG CS within dECM-based hydrogels, offering a novel bioengineering approach that is explored in the current study.

To complement a strategy based on dECM hydrogels, inclusion of the natural flavonoid, quercetin, has been shown in vivo to aid in chondrogenesis [42]. This molecule has been reported to influence cartilage tissue regeneration, exhibiting beneficial effects upon cells along with modulating inflammation [43, 44]. Also, it has been shown to provide a degree of crosslinking to collagen polymers, as an alternative to genipin [45, 46]. In a previous study by Greco et al. [45], the authors determined within decellularized dermal scaffolds (non-hydrogel), quercetin crosslinks collagen via interactions involving quercetin's hydroxyl groups and the amino groups of collagen [45]. Also, its inclusion within injectable alginate-based/bioglass hydrogels aided in chondrogenesis, along with inducing cartilage regeneration in an in vivo model [42]. To the best of our knowledge, the role of quercetin within dECM-based hydrogels or these functionalized with CS has not been reported, providing a novel avenue for experimentation.

Since the OA joint has a wide array of biochemical cues that may limit the success of any cell-seeded scaffolds, necessary functionalization approaches should be applied [47]. Notably, the significant loss of GAGs, including CS, is prominent in OA joints [12]. The absence of GAGs reduces the chondrogenic capacity of the ECM microenvironment [48]. Therefore, it adversely impacts the feasibility of using these biomaterials for tissue engineering approaches to tackle OA [48, 49]. Previous studies have applied functionalization strategies to produce biomaterials for a variety of applications [48, 50].

In the current study, we aimed to develop a novel hydrogel based on cartilage dECM functionalized with CS and containing

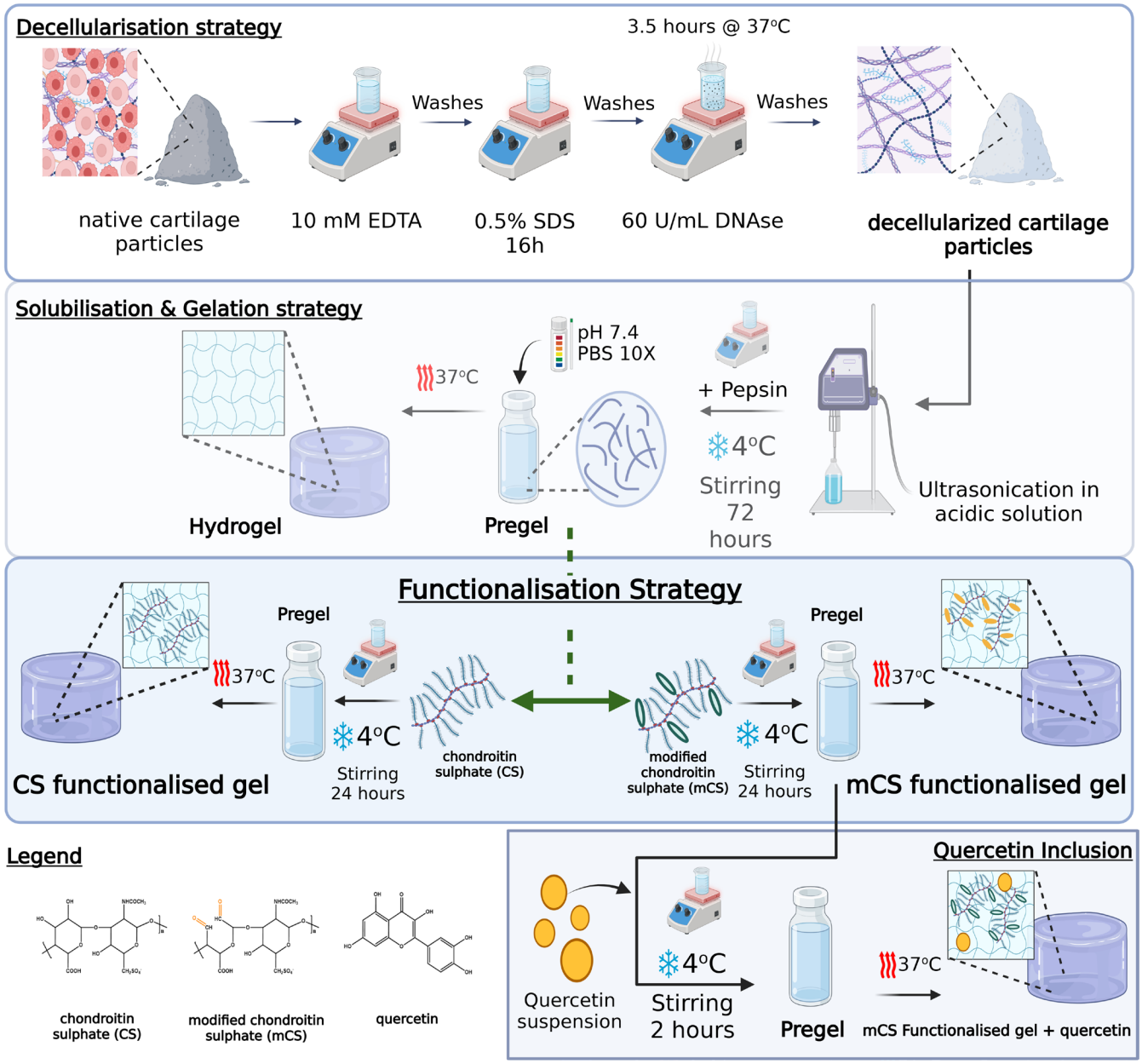

FIGURE 1 | Schematic of functionalized decellularised cartilage hydrogel production. Cartilage matrix was decellularised, milled, filtered, and solubilised into a pre-gel. This was used as a hydrogel or functionalized with either chondroitin sulphate (CS) or aldehyde modified chondroitin sulphate (mCS). Quercetin was also incorporated in the 0.4 mg/mL mCS hydrogel. Created in BioRender. Granja, P. (2025) https://BioRender.com/k5adszs.

quercetin (quercetin hydrate) to improve hydrogel properties and enhance chondrogenesis. The dECM pre-gels were functionalized using two approaches: (i) self-assembly with CS and (ii) modification of CS with aldehydes to provide a covalent functionalized hydrogel via formation of imine bonds. To further improve the hydrogel properties, we used quercetin, a pro-chondrogenic molecule (Figure 1). Using the different developed hydrogels led to similar cell viability as in dECM. While CS functionalization led to no significant changes in chondrogenic and hypertrophic gene expression, chondrocyte culture in quercetin-containing hydrogels significantly upregulated collagen type II. These results support dECM functionalization with aldehyde-modified chondroitin sulphate (mCS) and quercetin may promote a chondrogenic microenvironment for cartilage repair.

2 | Materials and Methods

2.1 | Harvesting Bovine Cartilage and Particle Production

Freshly cut bovine legs (approximately 1 year old) were obtained from Carnes Landeiro (Portugal), disinfected with 70% ethanol, with skin, ligaments, and muscle removed. Cartilage was harvested from articular joints with a scalpel and placed in

cold 1× phosphate buffered saline (PBS) containing 10% penicillin–streptomycin (Gibco, USA) and 5% Fungizone (Capricorn Scientific, Germany). Tissue slices were placed in a holder with optical temperature cutting compound (Kaltek srl, Italy), frozen in liquid nitrogen-cooled 2-methylbutane, and stored at −80°C until use. When required, these were thawed at room temperature (RT) and washed in 1× PBS for 6 cycles of 30 min. Excess solution was removed, and the slices were placed at −80°C, then freeze dried. The lyophilized slices were milled and filtered through an 800 μm sieve. The sieved dECM particles were collected and stored at −20°C until use.

2.2 | Decellularization Protocol

Native cartilage particles were thawed at RT and placed in Milli-Q (MQ) water containing 1% Pen/Strep (Gibco, USA), 0.5% Fungizone (Capricorn Scientific, Germany), and 0.1% Gentamycin (Gibco, Waltham, USA). The particles, at a concentration of 6 mg/mL, were stirred at RT for 15 min. The solution was removed at all stages of the protocol via centrifugation at 1300×*g* for 4 min, with the supernatant being removed. A 10 mM Tris-based hypotonic buffer (HB) containing 10 mM ethylenediaminetetraacetic acid (EDTA) at pH 7.8 was then added and allowed to stir for 22 h at RT. Following its removal, 1× PBS was added for 3 cycles of 1 h each. MQ water was then added to remove any excess salts for 5 min. A HB solution containing 0.5% sodium dodecyl sulphate (SDS) was introduced and allowed to stir for 16 h. To wash and remove the solution, 6 cycles of 15 min each of HB were required. To remove any excess salts, an MQ water wash was performed for 5 min. After centrifugation, 60 U/mL of DNAse enzymes in a solution containing 20 mM Tris and 2 mM $MgCl_2$ (pH 7.8) was employed for 3.5 h (37°C). This was then removed and washed for 3 cycles of 10 min with 1× PBS, followed by 3 cycles of 10 min with MQ water to remove salts. The remaining supernatant was removed, with the particles then being frozen and lyophilized to form the dECM particles.

2.3 | dsDNA Quantification

Lyophilized ECM and dECM particles underwent DNA extraction using the PureLink Genomic DNA Mini Kit (Invitrogen, USA) per manufacturer instructions. Particles were digested with Proteinase K in digestion buffer at 55°C for 4 h with occasional vortexing. The lysate was centrifuged to remove RNA, then mixed with ethanol and applied to a silica spin column. After washing, purified DNA was eluted. Double-strand deoxyribonucleic acid (dsDNA) was quantified using the PicoGreen assay per manufacturer's instructions, with fluorescence measured on a Synergy Mx microplate reader (BioTek, USA) at 480 nm excitation and 520 nm emission. Samples were run in duplicate with blanks and dual standard curves for DNA concentration, normalized to dry weight. The data were presented as ng deoxyribonucleic acid (DNA)/mg dry weight.

2.4 | Sulphated Glycosaminoglycan Quantification

The blyscan sulphated glycosaminoglycan (sGAG) (Biocolor, UK) assay was utilized to quantify sGAGs. The dry ECM and dECM particles were placed in a digestion solution (0.1 M sodium acetate, 0.01 M EDTA disodium salt, 0.005 M cysteine HCl, pH 6.4) containing 0.1 mg/mL of crystallized papain (Merck, USA). The samples digested for 12 h at 65°C, being stirred at 250 rpm. The kit quantifies sGAG by dye binding, pellet formation, and dye release for measurement. Absorbances were measured at 625 nm using a Synergy Mx microplate reader (BioTek, USA). Deionized water served as a reference and blank. sGAG concentration was determined from a standard curve, normalized for dilution and initial dry weight. The data were presented as μg sGAGs/mg dry weight.

2.5 | Aldehyde Modified Chondroitin Sulphate

Within an amber vial, 60.06 mg/mL of shark CS salt (Merck, USA) and 7.48 mg/mL of sodium periodate (NaIO4, Honeywell, USA) were dissolved in MQ water. Once dissolved, they were stirred for 6 h in the dark at RT, then dialyzed in a 1 kDa SpectraPor bag (Repligen, USA) against MQ water for 4 days with 3 daily changes of the solvent. Then filtered (0.22 μm), frozen, and freeze-dried with the mCS stored at −20°C until use.

2.6 | dECM Solubilization and Gelation

dECM particles were suspended in an amber vial with cold 3% acetic acid added at 80% FV (final concentration: 35 mg/mL). They were sonicated in ice using an ultrasonic liquid processor (FisherScientific, USA) with an amplitude of 20% and an ON/OFF cycle of 2/3 s (total ON cycle: 1 h). Then, 3200 units/mg pepsin powder (Merck, USA) was added (final concentration: 5 mg/mL), and the residual enzyme was suspended in the remaining 20% of cold 3% acetic acid to ensure the desired final concentration was reached. The mixture was stirred with a suitable magnet and rpm (to prevent foaming) for a total of 72 h.

Under cold conditions and utilizing cold solutions throughout, 10× PBS (10% FV) was added and vortexed gently, stirred at low rpm for 30 min. 10 M sodium hydroxide (NaOH) was added until the pH was approximately pH 7, the mixture was filtered to remove the undigested particles and allowed to centrifuge at 100 G for 1 min (4°C), ensuring maximum recovery. Then it was altered to pH 7.4 using 5 M NaOH. To undergo gelation, place the pre-gel at 37°C until complete gelation.

2.7 | Pre-Gel Functionalization

To fabricate the functionalized hydrogels, working stock mixtures produced were 1.0 mg/mL CS and 0.4 mg/mL mCS. Under cold conditions throughout, pre-gel solutions with either CS/mCS were stirred overnight (suitable rpm to prevent foaming). Diluted to 0.2 and 0.4 mg/mL, vortexed gently and stirred for 5 h to ensure homogeneity prior to use. 3.8 Inclusion of quercetin within functionalized hydrogels Quercetin (quercetin hydrate, MedChemExpress, USA) was dissolved in cold 1× PBS at a concentration of 12 mg/mL and then diluted to 6 mg/mL. Each was then added to 0.4 mg/mL mCS pre-gel at 2.5% FV (final concentration: 0.3 and 0.15 mg/mL). These were allowed to stir for 2 h at 4°C prior to use.

2.8 | Fourier Transform Infrared Spectroscopy Analysis

A fourier transform infrared spectroscopy (FTIR)-RAMAN Spectrometer 2000 (Perkin Elmer, USA) with: Universal attenuated total reflectance (ATR) sampling accessory and transmittance of solids (ToS) modules was used with 32 scans and a resolution of 4 cm^{-1}. To obtain the spectrum of CS and quercetin powders, these were dried overnight at RT under vacuum. Approximately 0.5–2 mg of each sample with 200 mg of potassium bromide were compressed into a pill and then read using the ToS module. The mCS and hydrogel-based solutions were read using the ATR module. Spectra were processed using the advanced baseline correction function provided by Spectragryph software.

2.9 | Rheological Analysis

Pre-gel samples were placed in a pre-warmed 37°C kinexus rheometer (Malvern Instruments, USA) with drops of water surrounding the centre platform to ensure humidity. The samples were allowed to stabilize and undergo gelation for 25 min. Ten samples per decade were recorded; first, a frequency sweep from 0.1 to 10 Hz with a strain of 1% (linear viscoelastic region (LVER) can be observed); second, with a fresh pre-warmed sample, a strain amplitude analysis with 1 Hz (within LVER) frequency and strain from 0.01% to 100%.

2.10 | Turbidity Measurements

Under cold conditions, pre-gel samples were prepared in duplicates and placed in a pre-cooled 96-well plate, with this being left on ice until further use. A Synergy Mx multi-mode microplate reader (BioTek, USA) was pre-warmed to 37°C. 100 μL of pre-gel solution of each condition was added as duplicates. The plate was left on a cold metal block until being placed in the plate reader with absorbances read every 31 s at a wavelength of 410 nm.

To normalize the absorbances as percentage turbidity, the method was adapted from a previous publication [51]. For the half-time gelation turbidity ($t_{1/2}$) calculations, linear interpolation between measured time points was undertaken when required.

2.11 | CryoSEM Preparation and Analysis

Pre-gels (50 μL) underwent full gelation at 37°C for 25 min. Then 200 μL MQ water at RT was delicately added above each hydrogel, being then placed at 7°C for 24 h. These observations were performed using a high-resolution scanning electron microscopy (SEM) with X-Ray Microanalysis with the following CryoSEM: JEOL JSM 6301F (JEOL Ltd., Japan), Oxford INCA Energy 350 (Oxford Instruments, UK), Gatan Alto 2500 (Gatan Inc., USA). After removing excess water, hydrogels were quickly cooled in sub-cooled nitrogen, transferred under vacuum to the chilled preparation chamber. The specimens were fractured and sublimated for 180 s at −90°C followed by being coated via Gold/Palladium sputtering for two 54 s cycles. Then samples were transferred into the SEM chamber (−150°C) with the images being then captured.

2.12 | Viability Analysis

Human mesenchymal stem cells (MSC) immortalized with human telomerase reverse transcriptase (hTERT) via lentiviral transfer were kindly provided by Prof. Matthias Schieker's group, Munich, Germany. Human dermal fibroblasts (HDF) were obtained commercially (ATCC, USA). The hTERT–MSCs or HDF were monolayer cultured in Dulbecco's modified eagle medium (DMEM) low glucose (-LG) medium (Gibco, USA), containing 10% fetal calf serum (FCS) (Gibco, USA or Corning, USA or Biowest, France), 100 U/mL penicillin, and 100 μg/mL streptomycin (Gibco, USA), being maintained at 37°C and a 5% CO_2 humidified environment. Either cell type was trypsinised and encapsulated within the hydrogel.

Cell seeding was undertaken via 4×10^5 cells/mL in a volume matching 2.5% FV of the pre-gel solution. Both solutions were combined under cold conditions and mixed using the pipette tip, up-down technique. 50 μL (containing 2×10^4 cells at a concentration of 4×10^5 cells/mL) of the mixed pre-gel solution for each condition was added as duplicates to a 96 well culture plate, undergoing gelation for approximately 8.5 min at 37°C within the incubator. The media was renewed with warm supplemented culture media and allowed to incubate for 75 min. The plates were then collected, the media renewed, and placed in the incubator overnight.

Stainings were conducted on days 1 and 3 after cell encapsulation. The cell media was replaced with culture media containing 2.4 μM Calcein AM (Thermofisher Scientific, USA) and 4.8 μM ethidium homodimer-1 (EthD-1) (Biotium, USA or Merck, USA), followed by incubation for 30 min. The media was carefully removed, and warm 1× PBS was added, then removed to wash away excess media. This was repeated, with excess liquid removed prior to imaging using a Keyence BZ-X810 microscope (Keyence Corporation, USA) or Operetta CLS (Perkin Elmer, USA). The day 3 plate should have media renewed on day 1 and repeat the same assay on day 3. Imaging was undertaken in 2 replicate gels per condition, for each independent experiment, quantified using Image J software, and results for replicate hydrogels were averaged.

2.13 | Chondrocyte Isolation

Process adapted from a previous protocol [52], describing the process to obtain human chondrocytes. Briefly, these were isolated from the cartilage of the caput femoris procured during endoprosthetic total hip arthroplasties at the Hospital Carl Gustav Carus Dresden. Both donors were female aged 62. Prior to surgical intervention, patients provided written informed consent and cell isolation approved by the ethics commission of TU Dresden.

Cartilage was harvested, sliced, and placed in Hanks' balanced salt solution (HBSS) (Gibco, USA) supplemented with 100 U/mL

penicillin and 100 μg/mL streptomycin (Gibco, USA) along with 2.5 μg/mL amphotericin B (Merck, USA). Here, using a scalpel, pieces were minced and placed in HBSS containing 1 mg/mL collagenase II (Merck, USA), being placed overnight on a shaker at 37°C. The solution was filtered through a 70 μm cell strainer (Corning, USA) with cells collected by centrifugation (5 min, 423 g). The cell pellet was resuspended in expansion media consisting of DMEM-LG with 10% FCS, 100 U/mL penicillin, and 100 μg/mL streptomycin (all from Gibco, USA). Also, 2.5 μg/mL amphotericin B was included only at this stage. These were then added to a cell culture flask and placed in an incubator (37°C, humidified atmosphere, and 5% CO_2). These were replenished twice a week with the expansion media and expanded to passage 3.

2.14 | Chondrogenic Differentiation

All chondrogenic experiments were undertaken as three independent experiments. Dedifferentiated chondrocytes at passage 3 were trypsinised and placed at a concentration of 2.4×10^6 cells/mL where it constituted 2.5% FV (pre-gel and cell suspension mixture) in chondrogenic medium. This medium contained DMEM high glucose (-HG) (Gibco, USA), 100 U/mL penicillin, 100 g/mL streptomycin, 1% ITS-X-Mix (Gibco, USA), 40 μg/mL proline, 50 μM ascorbic acid-2-phosphate, 10–7 M dexamethasone (all sourced from Merck, USA) and 10 ng/mL transforming growth factor β3 (Milteny Biotec, Germany).

97.5% FV of the pre-gel solution and 2.5% FV of cell suspension was mixed using the positive displacement pipette. 50 μL of the mixed solution (containing 1.2×10^5 cells: concentration of 2.4×10^6 cells/mL), each condition was added to a 96 well culture plate and underwent gelation for approximately 10 min at 37°C. Following this, warm supplemented DMEM-HG was added and allowed to incubate for 75 min. The media was renewed and placed in the incubator overnight. On days 1, 3, 5, and 7/8 post encapsulation, the media was renewed, being then renewed twice a week. On day 21, hydrogels were processed for further analysis (Sections 2.16–2.18).

2.15 | Histology

dECM and ECM were fixed in 4% paraformaldehyde in HBSS. Hydrogels with encapsulated cells were fixed in 4% phosphate buffered formaldehyde. These were paraffinized, sliced into 4 μm or 1.2 μm slices, respectively, deparaffinized, and stained using haemotoxylin and eosin (HE) or alcian blue staining. For DAPI staining, these were exposed to Spectral DAPI solution (AYOKA Biosciences, Marlborough, MA, USA), incubated for 5 min within a humidified chamber, followed by subsequent washing and mounting.

2.16 | RNA Extraction and cDNA Synthesis

Cell media was removed, and hydrogels were incubated with 3 mg/mL Collagenase type II (Merck, USA) in HBSS at 37°C for 1 h. Samples were centrifuged for 2 min at 250×g, the supernatant was removed, and cells were collected to undergo lysis. The lysis and RNA purification were undertaken following the manufacturer's protocol, either peqGOLD Microspin (VWR, USA) or ReliaPrepTM miRNA Cell and Tissue Miniprep System (Promega, USA) kits. The amount of RNA was determined using a Nanodrop spectrometer (Thermofisher Scientific, USA). The reverse transcriptase reaction was performed from 300 ng of total ribonucleic acid (RNA), utilizing the High Capacity cDNA Reverse Transcription kit (Applied Biosystems, USA) as per the manufacturer's instructions.

2.17 | Real Time Reverse Transcription-Polymerase Chain Reaction

Real-time polymerase chain reaction (RT-PCR) was used for quantifiable expression of chondrogenic and hypertrophic markers. It was evaluated using selected TaqMan Gene Expression Assay primers (Table 1) for chondrogenic markers (collagen type II (COL2A1), aggrecan (ACAN), cartilage oligomeric matrix protein (COMP)), along with hypertrophic markers (collagen type I (COL1A1), collagen type X (COL10A1), and alkaline phosphatase (ALPL)). The housekeeping gene utilized was β-actin (ACTB). Gene expression levels were assessed by quantifiable (Q) RT-PCR reaction via the cDNA from each sample with Taqman Fast Advanced Master Mix (Applied Biosystems, USA). All samples were run as duplicates for each gene while the normalized quantification was performed by using the comparative ΔΔCt method. The sample size was 6 for Figure 6, being 3 independent experiments with 2 biological replicates per condition, while for Figure 7, the sample size was 9, including 3 independent experiments with 3 biological replicates per condition.

2.18 | Statistical Analysis

Statistics were performed using GraphPad Prism (v8) and Excel software. Three independent experiments (minimum) were undertaken with the Shapiro–Wilk normality test used

TABLE 1 | Taqman primers utilized for the housekeeping, chondrogenic and hypertrophic genes.

Gene name	Gene symbol	Taqman assay ID
Aggrecan	ACAN	Hs00153936_m1
Beta-actin	ACTB	Hs01060665_g1
Alkaline phosphatase	ALPL	Hs01029144_m1
Cartilage oligomeric matrix protein	COMP	Hs00164359_m1
Collagen Type I alpha 1	COL1A1	Hs00164004_m1
Collagen Type II alpha 1	COL2A1	Hs00264051_m1
Collagen Type X alpha 1	COL10A1	Hs00166657_m1

to assess normal (Gaussian) distribution. dsDNA and GAG quantification were analyzed using paired t-test. $t_{1/2}$ and rheological data were analyzed using RM one-way ANOVA with Tukey correction (normally distributed data). Turbidity comparisons and cell viability analysis utilized RM two-way ANOVA with the Geisser–Greenhouse correction and Tukey's multiple comparisons test. Cell viability comparisons at the same time point utilized RM two-way ANOVA followed by Tukey's multiple comparisons test. Comparisons between time points used RM two-way ANOVA followed by Bonferroni's multiple comparison test. For the RT-PCR results, gene expression was analyzed as technical replicates generated from either three duplicate samples sourced from three (50 μL) cell-seeded hydrogels (Figure 6) or three triplicate samples, each from two (50 μL) cell-seeded hydrogels (Figure 7). The statistical analysis utilized the ΔCt data. All data groups were compared to each other using ordinary one-way ANOVA followed by Tukey multiple comparison (normally distributed data) or Kruskal-Wallis test followed by Tukey multiple comparison for (non-parametric data). The data are shown as fold changes (ΔΔCt) compared to the control (dECM) with upper and lower limits. Cell viability, gelation, and rheology spectra were analyzed using ordinary two-way ANOVA with Tukey's multiple comparison test.

3 | Results

3.1 | Cartilage Decellularization

To obtain a dECM-based hydrogel, we started by decellularizing native ECM particles using a combination of physical and enzymatic methods. After decellularization, both native ECM and dECM particles were evaluated to ascertain their DNA and GAG contents, providing insight into the decellularization efficiency in removing cellular material, while preserving ECM components. Since cartilage is extremely compact, cartilage particles (ca. 0.8 mm) were produced to increase the surface area and aid decellularization. Cartilage particles were subjected to combined chemical and enzymatic decellularization (Figure 1), resulting in the removal of virtually all cellular material (Figure 2A,B). This was confirmed by observing a porous structure within dECM particles that lacked or contained only remnants of cellular contents (Figure 2A). In relation to retaining the matrix components, the alcian blue results (Figure 2A, left images) appear to have a lighter blue stain observed in dECMs, showing loss of acidic polysaccharides including sGAGs. DAPI staining showed the cell nuclei in native cartilage particles, which were lost in dECM (Figure 2A, right images). Results for dsDNA quantification, depicted in Figure 2B, showed a significant decrease in the dECM, with 1.4 ng/mg, compared to the ECM particles with 224.2 ng/mg. The subsequent sGAG quantification (Figure 2C) showed a significant loss of 73% to approximately 87.3 μg/mg sGAG remaining in the dECM particles, compared with 324.2 μg/mg in the native ECM, caused by the decellularisation protocol.

Together, these results support that the decellularization was effective and the dECM was then used for further functionalization and incorporation.

3.2 | Production of Aldehyde Modified Chondroitin Sulphate

Then, to reintroduce the GAGs lost during the decellularization, we proceeded to incorporate CS in the decellularised ECM. We started by using sodium periodate (NaIO4) mediated oxidation of CS, which ensured the opening of the neighboring diols (—OH) located on the N-acetylgalactosamine residue, since the diols were converted, producing a dialdehyde functionalized derivative (Figure 3A). To preserve the CS original structure and properties, 0.3 M equivalents of sodium periodate ($NaIO_4$) were used to prevent excessive oxidation. To ensure the formation of aldehyde groups, FTIR analysis (Figure 3B) of the mCS and natural CS salt was performed. The new peak observed at 1738 cm^{-1} (Figure 3B) corresponded to the C—O stretch, suggesting the presence of aldehyde groups. The produced mCS was used to functionalise the dECM hydrogel to form the mCS hydrogels.

3.3 | Characterization of dECM-Based and Functionalised Hydrogels

To develop the ECM-based hydrogels, including functionalized hydrogels, a pre-gel solution was first obtained. After collecting the lyophilized dECM particles, the material was solubilized via treatment with 3% acetic acid under sonication. Following the addition of 10× PBS and neutralization with NaOH, along with filtration, a homogenous pre-gel without visible particles was produced, as depicted in Figure 4A. Also, this image shows that following thermogelation at 37°C, the pre-gel forms an opaque hydrogel. FTIR showed alterations within protein secondary structure following gelation, especially in the Amide I (1647 cm^{-1}), Amide II (1551 cm^{-1}), and Amide A stretching (3200–3500 cm^{-1}) regions, as shown in Figure 4B.

3.3.1 | Characterization of Functionalised Hydrogels With CS or mCS

Then, CryoSEM imaging was performed, since this approach prevents loss of the original gelatinous network structure, which occurs during normal SEM sample preparation. The representative images in Figure 4C indicate a fibrous network within the hydrogels, providing further evidence for having successfully produced a hydrogel.

Turbidity measurements allowed for gelation kinetics to be determined for the hydrogels developed following functionalization with different mCS concentrations (Figure 4D). The dECM hydrogel had the most efficient gelation kinetics, requiring a shorter period (6.0 min) to reach 50% turbidity, as shown in Figure 4E. In relation to the functionalized hydrogels, the 0.2 mg/mL mCS hydrogels required significantly more time to reach $t_{1/2}$, with 6.8 min.

Rheological analysis was performed to examine the viscoelastic properties and strength of the gelatinous network. When comparing the functionalized hydrogels to the control, it was observed both these had viscoelastic properties and solid-like hydrogel

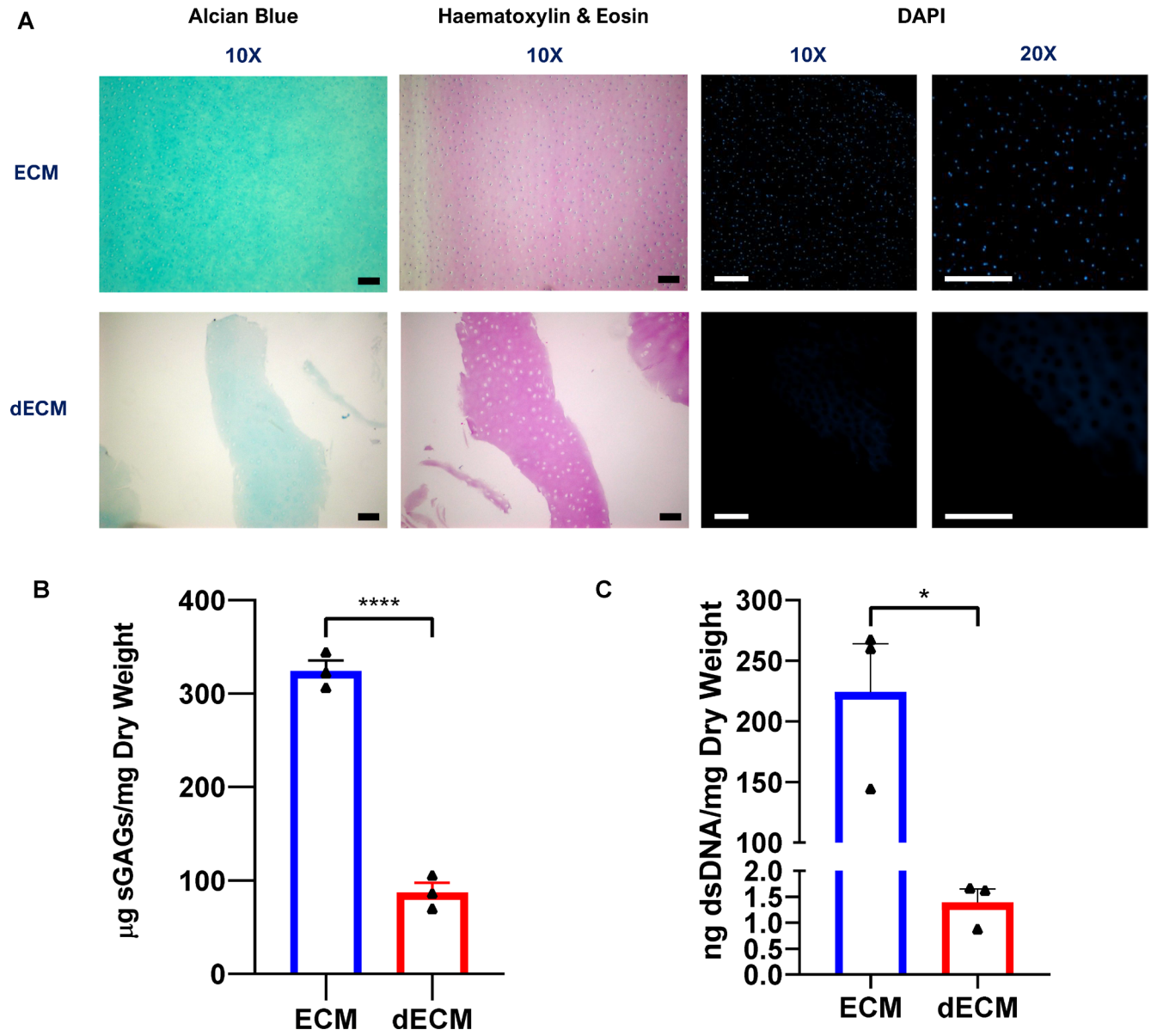

FIGURE 2 | Characterization of decellularized extracellular matrix. (A) Images of native and decellularized ECM cartilage particles stained with Alcian blue (GAGs), hematoxylin & eosin (matrix and cells), and DAPI (DNA). Images at 10× and 20× magnification with scale bars (100 μm for Alcian blue and H&E; 200 μm for DAPI). (B) Quantification of double-stranded DNA (dsDNA) in ECM and dECM particles. (C) Sulphated glycosaminoglycans (sGAGs) content quantified. Data shown as mean ± SEM ($n = 3$), with paired t-test significance indicated: $p < 0.05$ (*), $p < 0.0001$ (****). Symbols on the graph represent individual data points.

profiles (supplementary Figure S2). This was deduced due to the spectra showing storage modulus (G') being greater than the loss modulus (G''). As per Figure 4F–H, the G' and G'' of the hydrogels did not show any significant differences to each other at 0.1% strain. The lowest G' value (Figure 4F) recorded was 252.6 Pa for the 0.4 mg/mL mCS hydrogel; however, this was not significantly different to the dECM with a G' of 415.8 Pa. The G'' (Figure 4G) and complex modulus (G^*) (Figure 4H) also did not show any significant differences amongst the hydrogels. Overall, functionalizing the dECM pre-gel with the CS variants did not significantly alter the rheological characteristics with all hydrogels having a low G' and G'' modulus following CS functionalization.

The 0.4 mg/mL mCS hydrogel was selected to further understand the impact of incorporating quercetin. The CryoSEM representative images in Figure 5A, showed the organized fibrillar network within the hydrogels. The turbidity results in Figure 5B,C show that dECM hydrogels required 6.9 min to reach $t_{1/2}$ while in comparison the 0.15 mg/mL quercetin-incorporated hydrogels required significantly more time, taking 9.2 min. No significantly different $t_{1/2}$ times were observed when comparing the quercetin-incorporated hydrogels to 0.4 mg/mL mCS. In addition, comparing the quercetin concentrations also showed no significant differences.

The hydrogels had viscoelastic properties and were solid-like hydrogels at low strains and frequencies (supplementary Figure S3). Relative to 0.1% strain, the rheological data (Figure 5D) demonstrated that the G' of dECM hydrogel was 451.0 Pa, being significantly higher than the 0.4 mg/mL mCS, with a G' of 195.7 Pa.

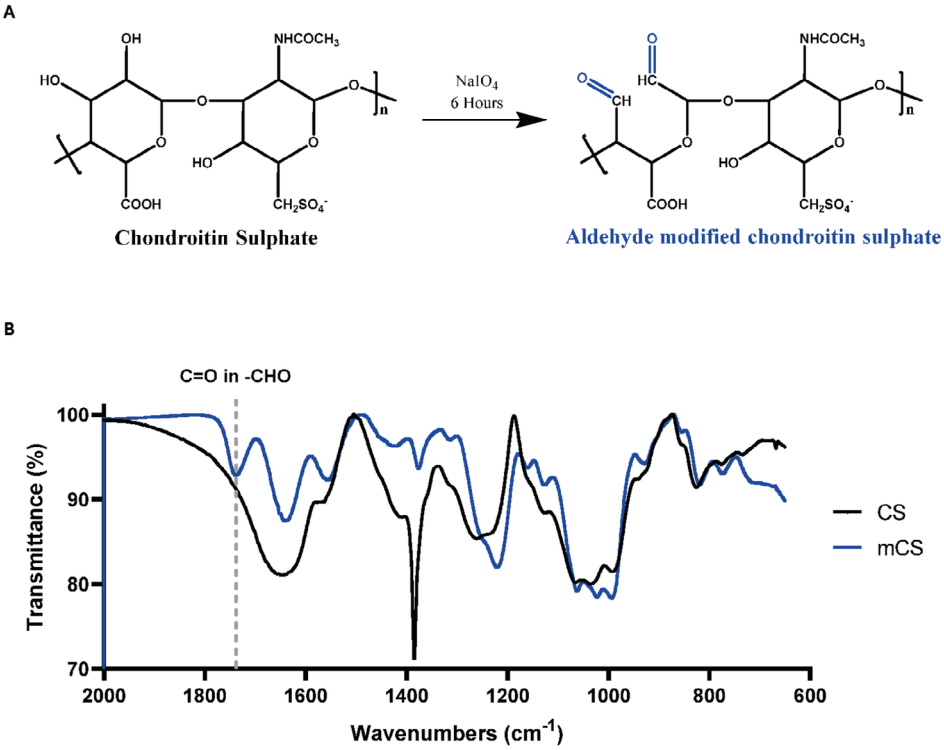

FIGURE 3 | Partial aldehyde modification of chondroitin sulphate. (A) Chemical structure of chondroitin sulphate salt before and after oxidation with 0.3 M equivalents of sodium periodate ($NaIO_4$) for 6 h, being then dialysed for 4 days, filtered (0.22 μm), and freeze-dried. (B) FTIR spectrum for chondroitin sulphate (CS) and aldehyde modified chondroitin sulphate (mCS). Spectra were zoomed in, allowing for the aldehyde peak to be observed at 1738 cm^{-1}.

Both quercetin-incorporated hydrogels had a G' that was not significantly different from each other and the dECM hydrogel. While the 0.3 mg/mL quercetin hydrogel had a G' of 405.0 Pa that was significantly different from the 0.4 mg/mL mCS hydrogel. In relation to the G'' (Figure 5E), the 0.4 mg/mL mCS hydrogel had an average value of 83.3 Pa, which was significantly different from the dECM gel, with 182.2 Pa. With no significant differences when comparing either hydrogel to either quercetin-incorporated hydrogel. To determine the strength of the hydrogels, the G* values at 0.1% strain were observed (Figure 5F). The 0.3 mg/mL quercetin hydrogel had a G* of 495.7 Pa, which was significantly different from 0.4 mg/mL mCS, with a G* of 213.9 Pa. The latter had a G* that was significantly different from the dECM hydrogel (486.9 Pa). However, there were no significant differences for the 0.15 mg/mL quercetin hydrogel in comparison to the rest of the hydrogels (Figure 5D–F).

Overall, our characterization analysis, showed 0.4 mg/mL mCS hydrogel to show significantly lower stiffness compared to dECM hydrogel.' to 'Overall, our characterization results showed that the 0.4 mg/mL mCS hydrogels have significantly lower stiffness, compared to dECM hydrogels.

3.4 | Biointerface Studies

Having produced a family of hydrogels, we proceeded to ascertain their impact on cell viability and chondrogenic differentiation.

To ascertain the viability of MSC within the developed hydrogels with the two concentrations of CS and mCS, a Calcein-AM and EthD-1 staining was undertaken at 1- and 3-days of MSC culture (Figure 6A–C). Representative images of the obtained results are illustrated in Figure 6A. The quantitative results presented in Figure 6B show the percentage of live cells in the total of live and dead cells for the different conditions. The dECM cell viability was around 70% and it remained consistent since the impact of the hydrogel functionalisation or time point provided no significant differences. Albeit, the hydrogels containing mCS show a slight decrease in cell viability at day 3 of culture (Figure 6B). To determine the impact of the developed hydrogels on chondrogenesis, MSC were cultured within the different hydrogels for 21 days. Histological stainings were performed with representative results presented in Figure 6C showing cells are widely distributed throughout the hydrogels and appear to maintain a relatively round morphology. The alcian blue staining shows similar staining intensities in the different conditions (Figure 6E). To gain a deeper understanding, both chondrogenic markers and hypertrophic marker related genes were analyzed. All conditions were compared to the control sample, the dECM hydrogel. The gene expression results for cartilage matrix proteins (COL2A1, ACAN and COMP) are depicted in Figure 6D–F, while hypertrophic markers (COL1A1, COL10A1, and ALPL), are depicted in Figure 6G–I. These showed relatively high variations between experiments but no statistically significant differences between dECM hydrogels and CS hydrogels.

Overall, there were no significant differences in cell behavior, upon functionalization with either CS or mCS in dECM hydrogels.

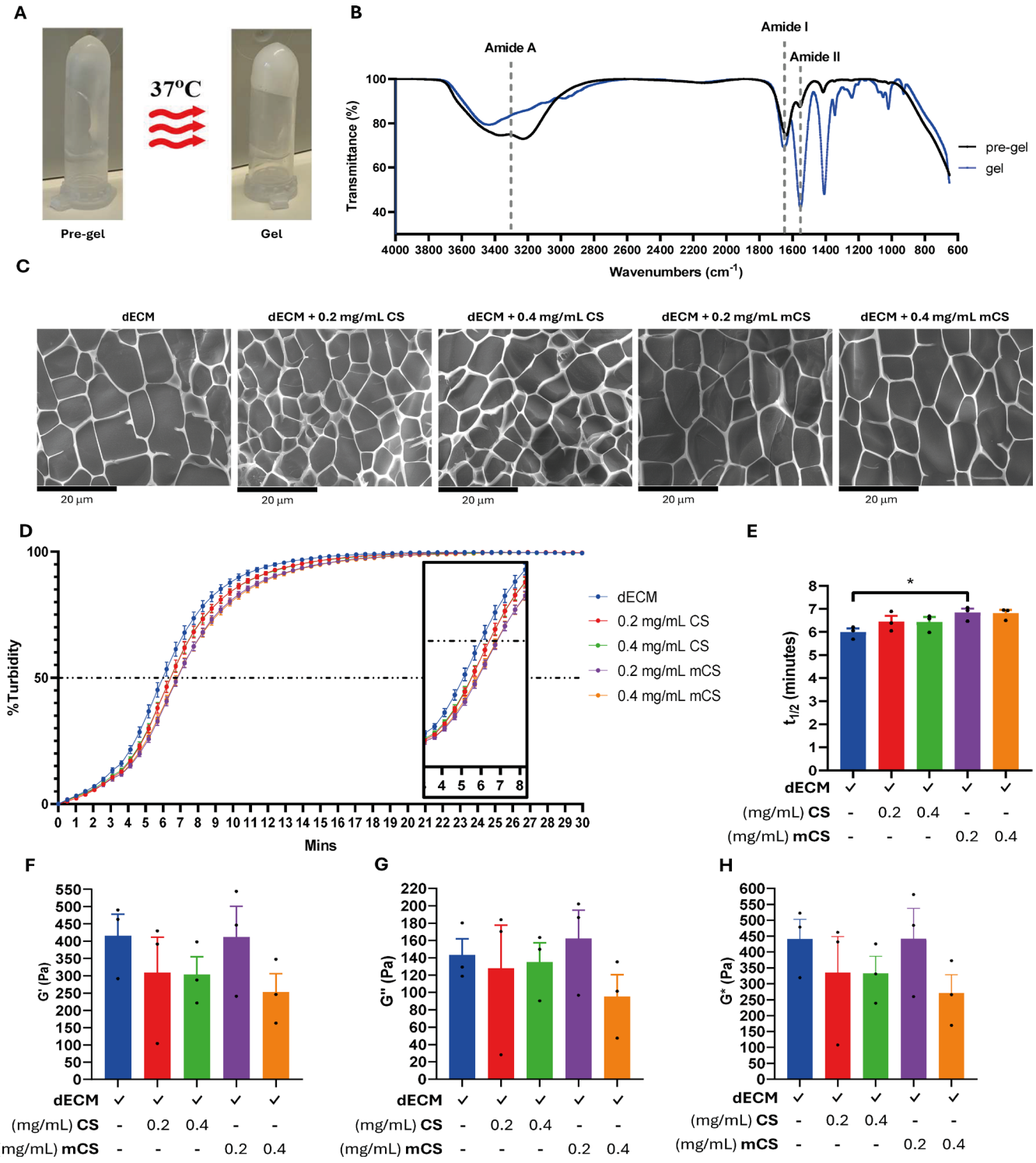

FIGURE 4 | Characterization of decellularized cartilage matrix and chondroitin sulphate-functionalized hydrogels. (A) Images of pre-gel solution and hydrogel. (B) FTIR spectra showing secondary structure formation. (C) CryoSEM analysis of decellularized matrix and functionalized hydrogels with either chondroitin sulphate (CS) and aldehyde modified chondroitin sulphate (mCS). Representative Images acquired utilizing ×2500 magnification with scale bars on the images. (D) Percentage turbidity of dECM with or without CS/mCS functionalization over time (minutes). (E) Time (minutes) to reach 50% maximum turbidity for each hydrogel. (F–H) Rheological results show at 0.1% strain (F) The average storage modulus (G'), (G) the loss modulus (G'') and (H) complex modulus (G^*) of the hydrogels. Data presented as average ± SEM ($n = 3$) with significant differences shown as $p < 0.05$ (*) with the p values being compared to dECM. Symbols on the graph represent individual data points.

To ascertain the ability of the developed hydrogels with incorporated quercetin to support cell culture, HDF cell viability was evaluated along time, using the Calcein-AM and EthD-1 staining (Figure 7A). Representative images show some dead cells in all experimental conditions, even in dECM (Figure 7A). Quantitative results are presented in Figure 7B

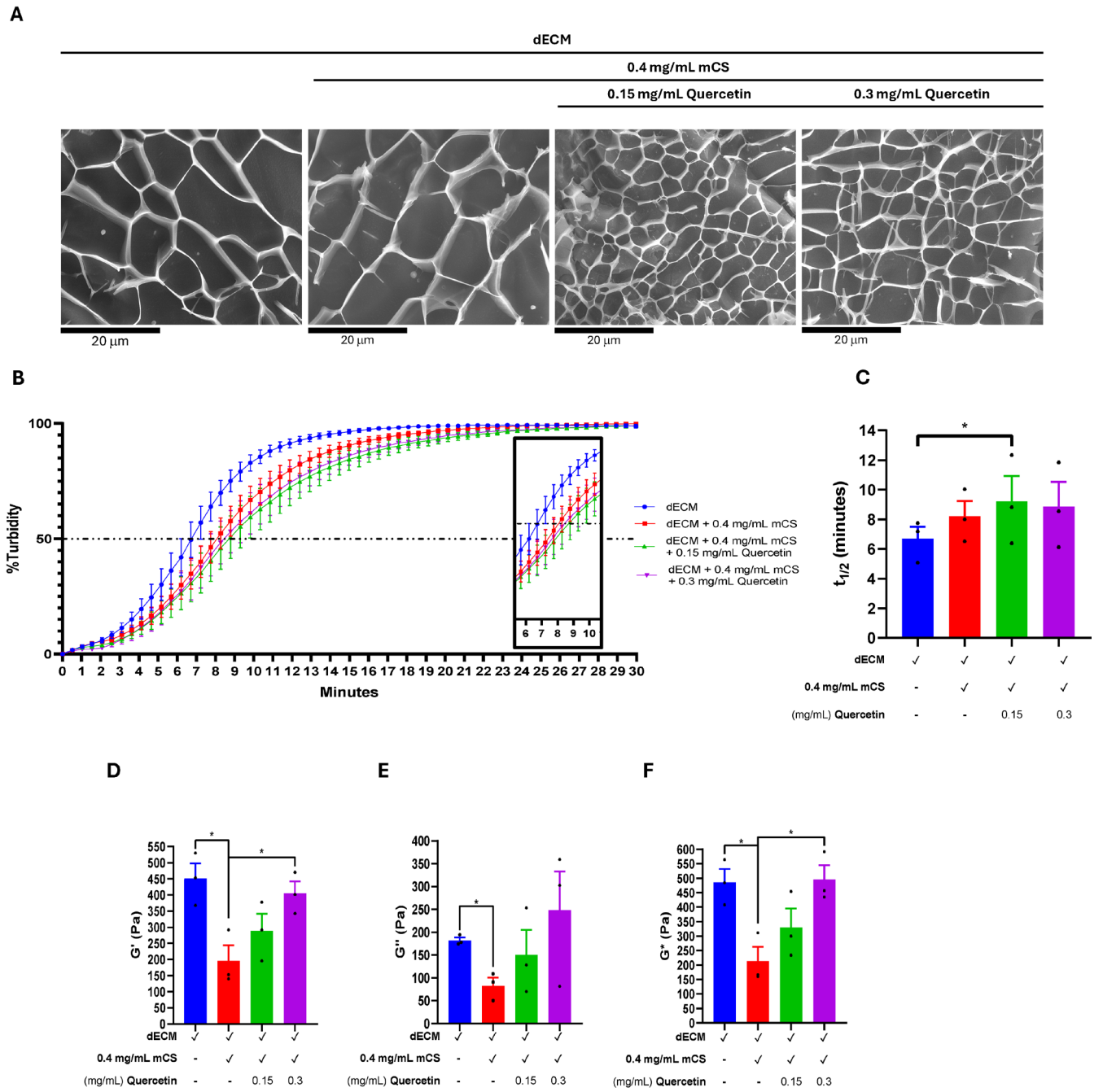

FIGURE 5 | Characterization of decellularized cartilage matrix and 0.4 mg/mL aldehyde-modified chondroitin sulphate hydrogels with or without quercetin. (A) CryoSEM analysis with representative images acquired utilizing ×2500 magnification (scale bars on images). (B) Percentage turbidity of decellularized matrix (dECM) functionalized with aldehyde-modified CS (mCS) with/without two quercetin concentrations (0.15 or 0.3 mg/mL) over time (minutes). (C) Time (minutes) to reach 50% maximum turbidity for the different hydrogels. Rheological results show at 0.1% strain (D) the average storage modulus (G'), (E) The loss modulus (G'') and (F) Complex modulus (G*) of the different hydrogels. Data presented as mean ± SEM ($n = 3$). Depending on the normal distribution, the statistical analysis undertaken either with (1) One-Way ANOVA test followed by Tukey's multi-comparison test and (2) Kruskal–Wallis test followed by Tukey's multi-comparison test $p < 0.05$ (*). In (B) statistical significance is against the dECM condition. Symbols on the graph represent individual data points.

and show no significant differences for cells cultured in 0.4 mg/mL mCS hydrogel between day 1 (66.0%) and 3 (65.7%). Also, cells cultured in hydrogels with 0.15 mg/mL quercetin showed similar viability as in the control hydrogel. While on day 1, the cells cultured in 0.3 mg/mL quercetin containing hydrogels showed a viability of 58.6%, which on day 3, reached a viability of 68.8%. However, the differences in cell viability were not significant.

Histological staining analysis showed well dispersed chondrocytes with a round morphology, while alcian blue staining did not show any significant differences when comparing to those

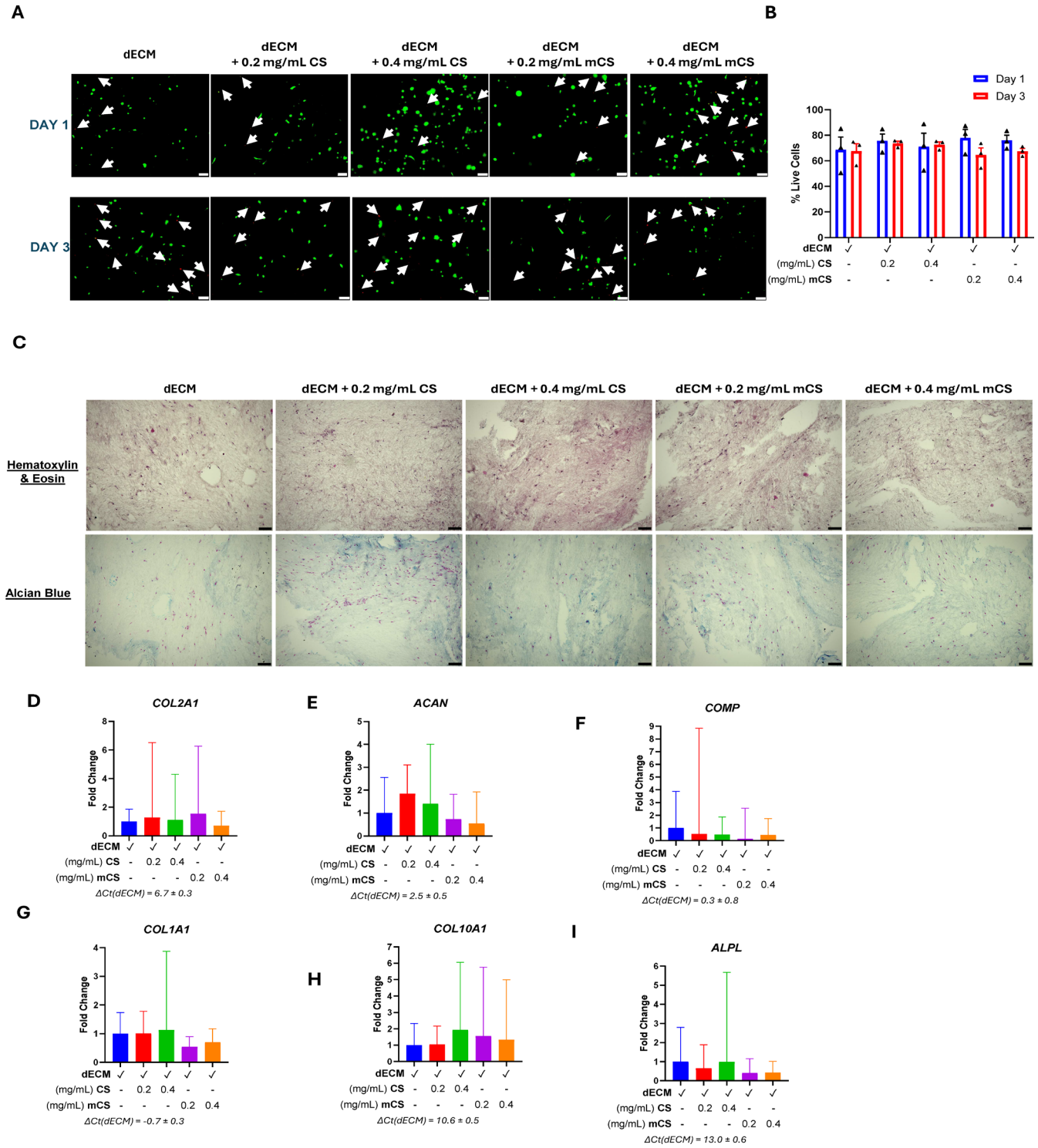

FIGURE 6 | MSC viability and chondrogenesis in both non- and functionalized hydrogel types. (A) Viability of hTERT-MSCs in decellularized matrix (dECM) and functionalized hydrogels, stained with Calcein AM (green, live) and Ethidium Homodimer-1 (red, dead) at days 1 and 3, with arrows pointing at examples of dead cells (10× magnification, 100 μm scale). (B) Percentage of viable cells shown as mean ± SEM ($n = 3$). (C) Hematoxylin & Eosin and Alcian blue staining of seeded hydrogels after 21 days in chondrogenic media (scale bars 100 μm). Symbols on the graph represent individual data points. (D–I) qRT-PCR analysis of ECM gene expression (COL2A1, ACAN, COMP, COL1A1, COL10A1, and ALPL) in seeded hydrogels after 21 days. Hydrogels tested included dECM with or without 0.2 or 0.4 mg/mL chondroitin sulphate (CS) or aldehyde-modified CS (mCS). Fold change (ΔΔCT) was calculated relative to dECM control. Error bars represent upper and lower limits ($n = 6$).

with incorporated quercetin (Figure 7C). Then, the effect of quercetin incorporation in 0.4 mg/mL mCS on chondrogenic gene expression of human chondrocytes was evaluated. Results indicate that incorporation of this compound, upregulated COL2A1 expression, when compared with 0.4 mg/mL mCS hydrogels, with results showing 6.6-fold increase for the lower

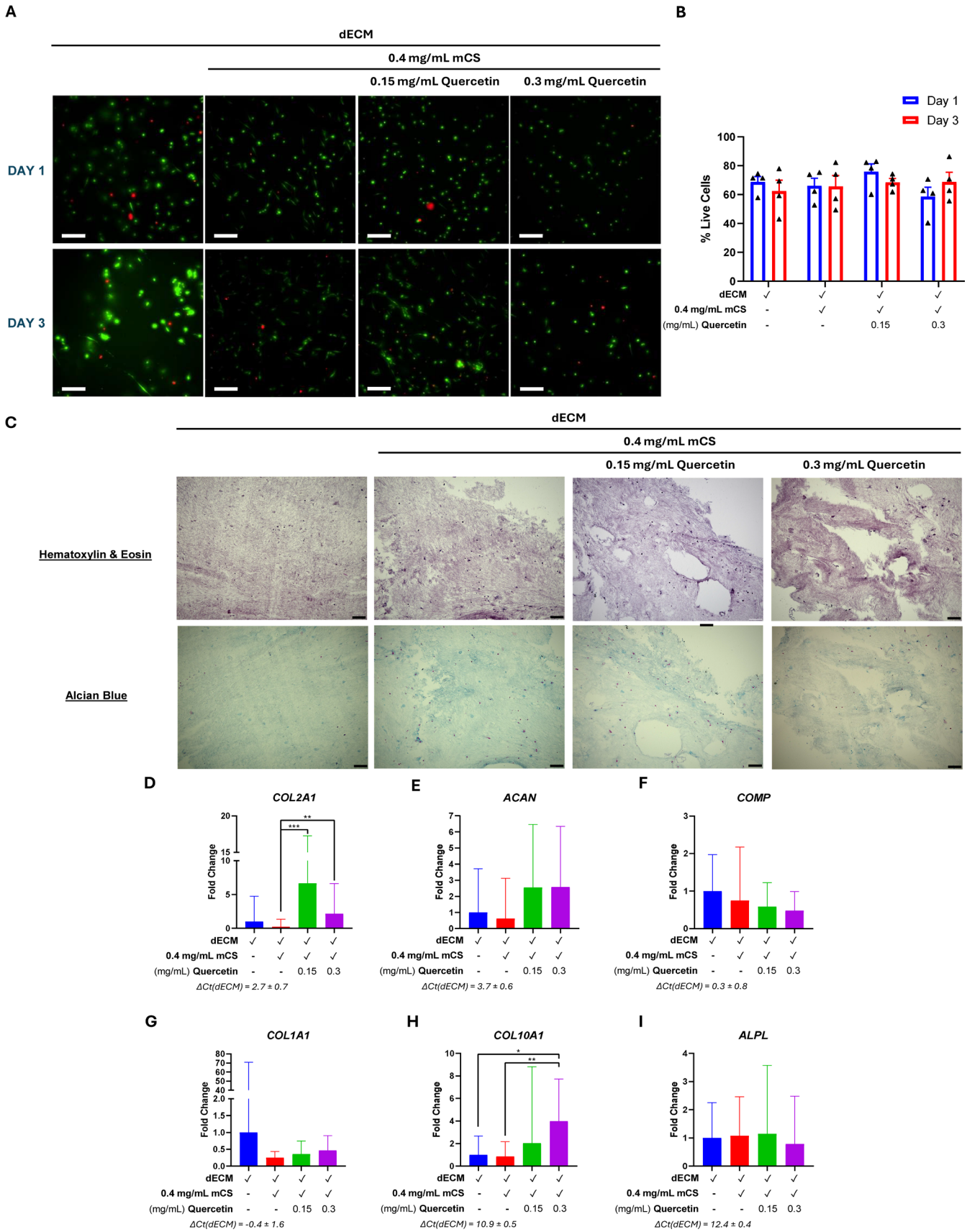

FIGURE 7 | Legend on next page.

FIGURE 7 | Cell viability and differentiation upon culture in non-functionalized and 0.4 mg/mL aldehyde modified chondroitin sulphate functionalized hydrogels with or without quercetin hydrate. (A) Viability of seeded human dermal fibroblasts (HDF) seeded in the different indicated hydrogels and stained with Calcien AM (green, live) and Ethidium Homodimer-1 (red, dead) at days 1 and 3. Scale bars = 200 μm. (B) Percentage of viable cells shown as mean ± SEM ($n = 4$). Symbols on the graph represent individual data points. (C) Hematoxylin & Eosin and Alcian blue staining of seeded hydrogels after 21 days in chondrogenic media (scale bars 100 μm). (D–I) qRT-PCR analysis of ECM gene expression (COL2A1, ACAN, COMP, COL1A1, COL10A1, and ALPL) in seeded hydrogels after 21 days. Hydrogels observed included that derived from dECM along with 0.4 mg/mL aldehyde modified chondroitin sulphate incorporated with quercetin at 0.15 and 0.3 mg/mL. Fold change (ΔΔCT) was calculated relative to dECM control. Error bars represent upper and lower limits ($n = 9$). Depending on the normal distribution, the statistical analysis undertaken either with (1) One-Way ANOVA test followed by Tukey's multi-comparison test and (2) Kruskal–Wallis test followed by Tukey's multi-comparison test $p < 0.05$ (*), $p < 0.01$ (**), $p < 0.001$ (***).

concentration while the higher concentration provided a 2.2-fold increase (Figure 7D). No significant differences were observed in ACAN and COMP expression (Figure 7E,F).

In relation to the hypertrophic markers, as per Figure 7G,I, both COL1A1 and ALPL gene expression were not significantly different amongst the hydrogels. For COL10A1 expression, the 0.3 mg/mL quercetin concentration, with a fold change of 4.0 (Figure 7H), showed a statistically significant increase when compared with dECM and 0.4 mg/mL mCS (0.9-fold). The lowest concentration of quercetin showed no significant differences, when compared to the other conditions. This demonstrates, 0.3 mg/mL quercetin and not the lower concentration of 0.15 mg/mL quercetin, in tandem with 0.4 mg/mL mCS can increase hypertrophic gene expression (COL10A1).

Overall, 0.15 mg/mL quercetin in 0.4 mg/mL mCS hydrogels enhances chondrogenic gene (COL2A1) expression.

4 | Discussion

New biomaterials capable of restoring cartilage structure and function are needed for OA patients. An ideal biomaterial should provide a microenvironment which closely mimics native cartilage. Therefore, cartilage dECM demonstrates potential for hydrogel and scaffold preparation, with benefits reported both in vitro and in vivo studies [32, 53]. Producing these biomaterials requires efficient ECM decellularization to minimize immunogenicity. Furthermore, detergent-based cell removal may disproportionately reduce certain GAGs, notably decreasing CS more extensively compared to the GAG hyaluronic acid (HA) [54, 55].

An undesirable result of decellularization is GAG loss, associated with the use of detergent-based solutions (e.g., SDS) [32]. This class of biopolymers, especially CS, is vital for chondrogenesis [56]. Thus, the ability to retain this polymer is paramount to ensure biomimicry [57]. Therefore, in this study, we re-introduced CS via functionalizing dECM, compensating for the loss occurring during decellularization. Our decellularization approach resulted in a retention of 87.3 μg/mg of sGAGs, a 73% decrease compared to the native cartilage (Figure 2C). In accordance with the literature, a reduced quantity of GAGs was to be expected, with Bordbar et al., reporting a decrease with 11 μg/mg of sGAGs remaining [32]. A subsequent paper by Guo and colleagues reported bovine articular cartilage contains approximately 40% GAGs, their dECM particle production utilizing SDS detergent resulted in a 62% decrease [58]. This study utilized a different sGAG quantification technique, 1,9-dimethylmethylene blue assay, showing higher initial sGAG levels than our results and Bordbar et al. [32, 58]. Despite GAG loss, dsDNA reduction to residual levels (Figure 1B) allowed progression to subsequent experiments aimed at compensating for this loss.

Considering the importance of sGAGs in chondrogenesis, reconstituting these appeared advantageous for enhancing hydrogel biomimicry [59]. This was explored via functionalizing dECM pre-gel with CS and evaluating physical versus covalent functionalization approaches. Physical functionalization entailed solely adding CS salt (shark sourced), allowing the polymers to self-assemble into an organized network during gelation, as previously reported [60]. While, covalent functionalization requires a CS modification, allowing the introduction of a complementary specific functional group to form a covalent bond with a chemical group within the dECM [24, 61]. An aldehyde modification was selected, as CS oxidation provides dialdehyde groups, enable multiple functional sites to be introduced [61, 62]. These can react with primary amines (imine bonds) or alcohols (hemiacetals) [62]. As previously reported, such modifications may impact the biopolymer's bioactivity and stability, along with high oxidiser concentrations associated with increased polymer chain cleavage [61, 62]. Thus, we exposed CS to low oxidiser levels to compare CS and mCS in cartilage dECM-based hydrogels.

Prior studies focused on CS functionalization of solid dECM scaffolds from tissues other than cartilage, using methacrylated CS hydrogels or CS impregnation, rather than hydrogels [60, 63, 64]. This is different to our approach, which involves directly functionalising the dECM-based pre-gel solution with CS or mCS. To our knowledge, CS functionalisation of dECM-derived hydrogels has not been previously shown, making our study a proof-of-concept.

Herein, the mCS modification was confirmed with FTIR analysis, and results are in agreement with previous reports [61]. Spectra showed a new peak at 1738 cm^{-1} correlating with the aldehyde (Figure 3B). Future studies may use varying amounts of oxidiser to produce different mCS variants and determine their corresponding hydrogel characteristics and biological behavior.

To convert a solid scaffold into a soluble pre-gel, a typical approach is performed using an acidic pepsin-containing solution.

Furthermore, since we wanted to maximize the retrieval of ECM components, ultrasonic waves were applied through a sonication process since Akram and colleagues had already demonstrated its ability to aid in maximizing the retrieval of collagen type II from cartilage [65]. Evidence from the literature shows ultrasonic waves result in mechanical oscillation and cavitation within the samples, disrupting protein structure [65, 66]. Such disruption can expose concealed protein regions, aiding in digestion [66]. Future studies should be undertaken to determine a more effective solubilization strategy, since difficulties were encountered in our experiments to ensure full solubilization of the dECM. Therefore, filtering was necessary to remove the insoluble material.

A concerning issue with dECM scaffolds is high batch-to-batch variability due to tissue source differences between animals of the same species [67]. Also, the solubilization process can introduce variability in the final product due to incomplete digestion leading to heterogeneous hydrogels [68]. To ensure consistency, standardized decellularization and solubilization protocols are needed to reduce batch-to-batch variability [67, 68]. In the current study, variability in characterization and biointerface results (Figures 4–7) reflects the use of different dECM batches.

Hydrogel mechanical properties were measured to assess the functionalization effect on viscoelasticity. The overall results show hydrogels with a low G' modulus, with dECM hydrogel having an initial modulus that was significantly different to the functionalized hydrogel, of 416 Pa (Figure 4F) According to a previous publication by Beck and colleagues [69], the compressive modulus for native articular cartilage is 1.8 MPa. While, the compressive and G' moduli measure different mechanical properties, the high level of difference, shows the hydrogel is considerably weaker than cartilage. Although no studies with dECM-based hydrogels functionalized with CS, could be found in the literature, our results appeared to correlate with a study undertaken by Stuart et al. [70], who have observed decreased G'' modulus following the presence of CS in collagen hydrogels [70]. While the G'' of the 0.4 mg/mL mCS hydrogel (Figure 5D), is significantly decreased versus the dECM hydrogel, supporting mCS hydrogels may follow this trend.

An objective of this research was also to determine how the network forms over time. Turbidity measurements showed decreased gelation kinetics for the functionalized hydrogels compared to the dECM hydrogel. The average $t_{1/2}$ (Figure 4E) showed the dECM hydrogel had the fastest gelation kinetics (6 min), with 0.2 mg/mL mCS hydrogels being significantly slower in comparison. Clearly, the mCS functionalization within these dECM hydrogels is hindering the network organization, slowing down gelation efficiency.

The viability of cells in the CS modified hydrogels was evaluated at day 1 and day 3 of culture. These early time points were selected to deduce the effect of cells being exposed to a hydrogel containing 0.5 M sodium acetate. The presence of this salt is a direct result of utilizing NaOH to neutralize the 3% acetic acid pepsin containing solution used during the dECM solubilization. Such a concentration of the resulting 0.5 M sodium acetate may lead to lower cellular viability according to previous studies [35]. Second, these time points allowed for ascertaining the cell viability of mCS functionalized hydrogels, which contained aldehyde modified CS. Such functional groups can interact with cellular components, disrupting cellular processes, resulting in toxicity which impacts cellular viability [71]. Overall, these time points showed there is only mild cytotoxicity to the seeded cells, at both day 1 and day 3 for all hydrogels (Figure 6A,B), with no significant differences when comparing the conditions. Therefore, cell viability of 70% is a potential limitation of our study. Also, the number of cells appears to show some variations (Figure 6A) especially between day 1 and 3. Previous studies have reported at week 6, a beneficial impact in cell viability when CS was provided to 3D cell cultures [50]. No similar significant effects were observed within our study at day 1 and 3. Perhaps the composition or low stiffness of our dECM hydrogels nullifies the beneficial effect upon cell viability provided by CS. Furthermore, since we had to decellularize the cartilage ECM, this can modify the biochemical and structural integrity of the ECM components [72]. This may be associated with the cytotoxicity observed within the hydrogels including the dECM-based hydrogel. A study by Bordbar and colleagues reported that rabbit bone marrow stem cells exhibited lower metabolic activity (an indirect measurement of cell viability) at day 7 within cartilage dECM hydrogels compared to dECM solid scaffolds. Also, all conditions showed higher activity at day 7 compared to day 3, with the dECM hydrogel showing the slowest cell growth [32]. While, in our study, cell viability was directly measured (counting live and dead cells), with mild cytotoxicity observed in the dECM hydrogel. Evidently, in both the previous study and our results show no significant differences at 3 days. Although later time points were not investigated in our study, the early-stage data provided valuable insight into initial cell responses to these hydrogels and functionalization strategies.

Hydrogel mechanical cues, especially stiffness, can influence MSC chondrogenic differentiation [73]. However, in contrast to our initial hypothesis on the effect of CS functionalisation, the expression of chondrogenic and hypertrophic genes showed no significant differences overall (Figure 6D–I). A previous study by Bachmann and colleagues [74] showed a stiffness of 30 kPa compared to 1 kPa that resulted in increased collagen type II and aggrecan synthesis [74]. Since in our study we have hydrogels presenting low stiffness, this may play a role in the results obtained in suppressing cartilage matrix production. Finally, it should be ascertained in future studies if hydrogel stiffness or CS has a preponderant impact on chondrogenesis induced by dECM hydrogels. A study by Ai et al. [73] has shown the optimal CS concentration for chondrogenesis was 6% (w/v) regardless of the stiffness of hydrogels, but for the same CS concentration stiffer hydrogels tend to have better performance [73]. Perhaps investigating further CS concentration and improving dECM hydrogel stiffness via crosslinking may allow CS functionalization to effectively enhance the microenvironment's chondrogenic ability.

Furthermore, our approach utilized a chondrogenic supplemented culture medium. This was due to having MSC or dedifferentiated chondrocytes which necessitate supplements to undergo re-differentiation to express cartilage specific genes [75]. Consequently, any changes in the expression of chondrogenic genes are not only influenced by the biochemical and

biomechanical microenvironment provided by the hydrogel, but also by these factors. To assess the direct impact of the hydrogels, removing chondrogenic supplementation, as demonstrated by Roncada et al., could provide valuable insights [76]. However, supplementation is considered necessary for the activation of the chondrogenic signaling pathways [77], and thus was selected.

This study also examined quercetin's influence upon hydrogel mechanical and biological behavior, since it has been shown to crosslink collagen and support chondrogenesis [42, 45]. However, no previous studies have been published focusing on its use within dECM-based hydrogels.

Rheological data for quercetin-incorporated hydrogels demonstrated its ability to improve the G' modulus. This aligns with previous studies on evaluating quercetin's crosslinking ability [45]. The G* analysis in Figure 5F provides evidence that 0.3 mg/mL quercetin incorporated within 0.4 mg/mL mCS significantly increases the hydrogel's strength (0.3 mg/mL quercetin vs. 0.4 mg/mL mCS), while not showing significant differences to the dECM hydrogel. This can imply that incorporated quercetin within the dECM and 0.4 mg/mL mCS hydrogel restored the mCS functionalized hydrogels to their original strength prior to functionalisation (since no significant differences between quercetin concentrations and dECM). Thus, it depicts the importance of quercetin for improving mCS hydrogel's rheological properties. However, no significant difference was observed between quercetin-incorporated hydrogels and its corresponding hydrogel, 0.4 mg/mL mCS. In a previous publication by Greco et al. [45], incorporation of 1 mg/mL of quercetin (in PBS) in decellularized dermal scaffolds increased their stiffness, though less than crosslinking with genipin [45]. Our results may suggest that quercetin can overcome the hindrances that mCS provides to the hydrogel network, allowing for improved rheological properties. In our current study, we are limited to observing the influence of quercetin in a specific mCS hydrogel. It may be necessary and of great importance to analyze the influence in the remaining CS gels and dECM-based hydrogel.

Quercetin exhibits anti-cancer cytotoxicity against hTERT-mutated cells [78, 79]. Therefore, HDF cells, which tolerate quercetin, were used in these experiments [80]. Results in Figure 7A,B showed that quercetin incorporation within the 0.4 mg/mL mCS-functionalized hydrogels did not lead to significant increases in cytotoxicity (as can potentially occur with hTERT cell lines). However, these all showed low to moderate cytotoxicity when observing both day 1 and day 3, which constitutes a potential limitation of the current study. A previous study by Zawani and colleagues used quercetin-embedded gelatin–elastin hydrogels and showed HDF cell viability at day 1 was optimal with 0.125 mg/mL quercetin [81]. Their results report cell viability via a cell metabolic assay rather than directly quantifying the percentage of live cells as in this study. Our quercetin-incorporated hydrogels that had the highest viability at day 1 were 0.15 mg/mL (75.9%), which corresponds to mild cytotoxicity and was not statistically different from the rest of the conditions. Notably, the results in our study could possibly be associated with the inherent properties of the dECM hydrogel contributing to the observed cytotoxicity. Also, Greco and colleagues reported that 1 mg/mL quercetin is optimal for crosslinking, while Zawani and colleagues found that cell viability is preferable at concentrations below 0.5 mg/mL [45, 81]. To minimize cytotoxicity, we limited the highest quercetin concentration to below 0.5 mg/mL. Despite this, cytotoxicity was still observed, which may have influenced the chondrogenesis-related results.

The gene expression results show quercetin inclusion provides statistically significant advantages (especially when comparing the 0.4 mg/mL mCS hydrogel +/− quercetin) relative to the expression of COL2A1. The 0.15 mg/mL quercetin-incorporated hydrogel showed the highest significant increase (6.6-fold change) vs. 0.4 mg/mL mCS hydrogel (0.2-fold change) seen in Figure 7D. Increased COL2A1 has been previously reported in rat chondrocytes affected by quercetin-bioglass hydrogels [41]. Both quercetin concentrations significantly increased COL2A1 expression. There was a significant increase in the hypertrophic gene COL10A1, with 0.3 mg/mL quercetin showing a 4.0-fold increase (Figure 7H) versus both the dECM hydrogel and 0.4 mg/mL mCS-functionalized dECM hydrogel. Since the percentage of live cells at day 1 for 0.3 mg/mL quercetin showed moderate cytotoxicity, this could have implications in the results (COL10A1). Together, these results show 0.4 mg/mL mCS hydrogels have a positive influence upon chondrogenesis (> hypertrophy) when quercetin is incorporated, especially at 0.15 mg/mL. Therefore, providing a basis for future studies to apply quercetin for enhancing the chondrogenic regenerative capability of CS functionalised dECM.

5 | Conclusion

Cartilage dECM-derived hydrogels showed no significant differences in rheological behavior, gelation kinetics, or biointerface effects compared to CS/mCS-functionalized hydrogels. The inclusion of quercetin in 0.4 mg/mL mCS-functionalized dECM hydrogels appears to enhance COL2A1 expression. Therefore, this study presents a proof-of-concept hydrogel that combines mCS and quercetin to enhance chondrogenesis. Future work should investigate CS and further mCS concentrations for dECM hydrogel functionalization along with quercetin's interaction with CS/mCS. This will allow for the identification of an optimal formulation for chondrogenesis and clinical use.

Acknowledgments

The authors thank the i3s scientific platforms: Histology, Bioimaging, and Advanced Biomaterials Characterization; Daniela Silva (CEMUP) for Cryo SEM imaging; Suzanne Manthey and Annett Wenke (TFO group) for histologic sample preparation; and Emily Fichter, Johanna Bellstedt, Max von Witzleben, Richard Richter, Ricardo Vidal, Rui Pereira, and Carlos Redondo.

Conflicts of Interest

The authors declare no conflicts of interest.

Data Availability Statement

The data that support the findings of this study are available from the corresponding author upon reasonable request.

References

1. J. D. Steinmetz, G. T. Culbreth, L. M. Haile, et al., "Global, Regional, and National Burden of Osteoarthritis, 1990-2020 and Projections to 2050: A Systematic Analysis for the Global Burden of Disease Study 2021," *Lancet Rheumatology* 5, no. 9 (2023): E508–E522, https://doi.org/10.1016/S2665-9913(23)00163-7.

2. S. Koushesh, S. M. Shahtaheri, D. F. McWilliams, et al., "The Osteoarthritis Bone Score (OABS): A New Histological Scoring System for the Characterisation of Bone Marrow Lesions in Osteoarthritis," *Osteoarthritis and Cartilage* 30 (2022): 746–755, https://doi.org/10.1016/j.joca.2022.01.008.

3. K. Liu, B. J. Zhang, and X. L. Zhang, "Promoting Articular Cartilage Regeneration Through Microenvironmental Regulation," *Journal of Immunology Research* 2024 (2024): 1–16, https://doi.org/10.1155/2024/4751168.

4. J. Eschweiler, N. Horn, B. Rath, et al., "The Biomechanics of Cartilage-An Overview," *Life* 11, no. 4 (2021): 14, https://doi.org/10.3390/life11040302.

5. M. Loparic, D. Wirz, A. U. Daniels, et al., "Micro- and Nanomechanical Analysis of Articular Cartilage by Indentation-Type Atomic Force Microscopy: Validation With a Gel-Microfiber Composite," *Biophysical Journal* 98, no. 11 (2010): 2731–2740, https://doi.org/10.1016/j.bpj.2010.02.013.

6. N. V. Jaumard, W. C. Welch, and B. A. Winkelstein, "Spinal Facet Joint Biomechanics and Mechanotransduction in Normal, Injury and Degenerative Conditions," *Journal of Biomechanical Engineering* 133, no. 7 (2011): 71010, https://doi.org/10.1115/1.4004493.

7. S. A. O'Leary, J. M. Link, E. O. Klineberg, J. C. Hu, and K. A. Athanasiou, "Characterization of Facet Joint Cartilage Properties in the Human and Interspecies Comparisons," *Acta Biomaterialia* 54 (2017): 367–376, https://doi.org/10.1016/j.actbio.2017.03.017.

8. G. C. de Campos, R. Mundi, C. Whittington, M.-J. Toutounji, W. Ngai, and B. Sheehan, "Osteoarthritis, Mobility-Related Comorbidities and Mortality: An Overview of meta-Analyses," *Therapeutic Advances in Musculoskeletal Disease* 12 (2020): 1759720X20981219, https://doi.org/10.1177/1759720X20981219.

9. Y. H. Liao, Y. Ren, X. Luo, et al., "Interleukin-6 Signaling Mediates Cartilage Degradation and Pain in Posttraumatic Osteoarthritis in a Sex-Specific Manner," *Science Signaling* 15, no. 744 (2022): eabn7082, https://doi.org/10.1126/scisignal.abn7082.

10. M. Morgan, J. Thai, V. Nazemian, R. Song, and J. J. Ivanusic, "Changes to the Activity and Sensitivity of Nerves Innervating Subchondral Bone Contribute to Pain in Late-Stage Osteoarthritis," *Pain* 163, no. 2 (2022): 390–402, https://doi.org/10.1097/j.pain.0000000000002355.

11. J. Sheng, D. Liu, X. Kang, Y. Chen, K. Jiang, and W. Zheng, "Egr-1 Increases Angiogenesis in Cartilage via Binding Netrin-1 Receptor DCC Promoter," *Journal of Orthopaedic Surgery and Research* 13 (2018): 125, https://doi.org/10.1186/s13018-018-0826-x.

12. E. A. Aisenbrey and S. J. Bryant, "The Role of Chondroitin Sulfate in Regulating Hypertrophy During MSC Chondrogenesis in a Cartilage Mimetic Hydrogel Under Dynamic Loading," *Biomaterials* 190 (2019): 51–62, https://doi.org/10.1016/j.biomaterials.2018.10.028.

13. C. J. Lian, C. Lian, X. Wang, et al., "Collagen Type II Suppresses Articular Chondrocyte Hypertrophy and Osteoarthritis Progression by Promoting Integrin 1-SMAD1 Interaction," *Bone Research* 7 (2019): 8, https://doi.org/10.1038/s41413-019-0046-y.

14. J. S. Kim, M. H. Ali, F. Wydra, et al., "Characterization of Degenerative Human Facet Joints and Facet Joint Capsular Tissues," *Osteoarthritis and Cartilage* 23, no. 12 (2015): 2242–2251, https://doi.org/10.1016/j.joca.2015.06.009.

15. P. I. Mapp and D. A. Walsh, "Mechanisms and Targets of Angiogenesis and Nerve Growth in Osteoarthritis," *Nature Reviews Rheumatology* 8 (2012): 390–398, https://doi.org/10.1038/nrrheum.2012.80.

16. E. P. Pourmand, I. Binderman, S. B. Doty, V. Kudryashov, and A. L. Boskey, "Chondrocyte Apoptosis Is Not Essential for Cartilage Calcification: Evidence From an in Vitro Avian Model," *Journal of Cellular Biochemistry* 100, no. 1 (2007): 43–57, https://doi.org/10.1002/jcb.20977.

17. O. O. WM, C. Little, V. Duong, and D. J. Hunter, "The Development of Disease-Modifying Therapies for Osteoarthritis (DMOADs): The Evidence to Date," *Drug Design, Development and Therapy* 15 (2021): 2921–2945, https://doi.org/10.2147/DDDT.S295224.

18. Q. S. Shen, Y. Guo, K. Wang, C. Zhang, and Y. Ma, "A Review of Chondroitin Sulfate's Preparation, Properties, Functions, and Applications," *Molecules* 28, no. 20 (2023): 7093, https://doi.org/10.3390/molecules28207093.

19. R. J. Elliott and D. L. Gardner, "Changes With Age in the Glycosaminoglycans of Human Articular Cartilage," *Annals of the Rheumatic Diseases* 38, no. 4 (1979): 371–377, https://doi.org/10.1136/ard.38.4.371.

20. A. M. Hitchcock, K. E. Yates, S. Shortkroff, C. E. Costello, and J. Zaia, "Optimized Extraction of Glycosaminoglycans From Normal and Osteoarthritic Cartilage for Glycomics Profiling," *Glycobiology* 17, no. 1 (2007): 25–35, https://doi.org/10.1093/glycob/cwl046.

21. A. L. da Cunha, L. G. de Oliveira, L. F. Maia, L. F. de Oliveira, Y. M. Michelacci, and J. A. de Aguiar, "Pharmaceutical Grade Chondroitin Sulfate: Structural Analysis and Identification of Contaminants in Different Commercial Preparations," *Carbohydrate Polymers* 134 (2015): 300–308, https://doi.org/10.1016/j.carbpol.2015.08.006.

22. K. R. Yang, M. F. Tsai, C. J. Shieh, et al., "Ultrasonic-Assisted Extraction and Structural Characterization of Chondroitin Sulfate Derived From Jumbo Squid Cartilage," *Food* 10, no. 10 (2021): 2363, https://doi.org/10.3390/foods10102363.

23. SER Hernandez, I Streeter, and de Leeuw, "The Effect of Water on the Binding of Glycosaminoglycan Saccharides to Hydroxyapatite Surfaces: A Molecular Dynamics Study," *Physical Chemistry Chemical Physics* 17, no. 34 (2015): 22377–22388, https://doi.org/10.1039/c5cp02630j.

24. D. A. Wang, S. Varghese, B. Sharma, et al., "Multifunctional Chondroitin Sulphate for Cartilage Tissue-Biomaterial Integration," *Nature Materials* 6, no. 5 (2007): 385–392, https://doi.org/10.1038/nmat1890.

25. H. Cao and S. Y. Xu, "EDC/NHS-Crosslinked Type II Collagen-Chondroitin Sulfate Scaffold: Characterization and in Vitro Evaluation," *Journal of Materials Science: Materials in Medicine* 19, no. 2 (2008): 567–575, https://doi.org/10.1007/s10856-007-3281-5.

26. J. Q. Chen, J. Chen, J. Yang, et al., "Modified Hyaluronic Acid Hydrogels With Chemical Groups That Facilitate Adhesion to Host Tissues Enhance Cartilage Regeneration," *Bioactive Materials* 6, no. 6 (2021): 1689–1698, https://doi.org/10.1016/j.bioactmat.2020.11.020.

27. R. Edmondson, J. J. Broglie, A. F. Adcock, and L. Yang, "Three-Dimensional Cell Culture Systems and Their Applications in Drug Discovery and Cell-Based Biosensors," *Assay and Drug Development Technologies* 12, no. 4 (2014): 207–218, https://doi.org/10.1089/adt.2014.573.

28. X. J. Wang, W. He, H. Huang, et al., "Recent Advances in Hydrogel Technology in Delivering Mesenchymal Stem Cell for Osteoarthritis Therapy," *Biomolecules* 14, no. 7 (2024): 858, https://doi.org/10.3390/biom14070858.

29. M. Dussoyer, A. Michopoulou, and P. Rousselle, "Decellularized Scaffolds for Skin Repair and Regeneration," *Applied Sciences* 10, no. 10 (2020): 3435, https://doi.org/10.3390/app10103435.

30. Z. F. Murtaza, A. Abou Fares, F. AlMuhairi, et al., "A Bioengineered Model for Reinnervating the Decellularized Extracellular Matrix of Corneal Scaffolds," *Medical Hypotheses* 185, no. 2024 (2024): 111315, https://doi.org/10.1016/j.mehy.2024.111315.

31. X. Y. Wang, A. Shakeel, A. E. Salih, et al., "A Scalable Corneal Xenograft Platform: Simultaneous Opportunities for Tissue Engineering and Circular Economic Sustainability by Repurposing Slaughterhouse Waste," *Frontiers in Bioengineering and Biotechnology* 11 (2023): 1133122, https://doi.org/10.3389/fbioe.2023.1133122.

32. S. Bordbar, N. Lotfi Bakhshaiesh, M. Khanmohammadi, F. A. Sayahpour, M. Alini, and M. Baghaban Eslaminejad, "Production and Evaluation of Decellularized Extracellular Matrix Hydrogel for Cartilage Regeneration Derived From Knee Cartilage," *Journal of Biomedical Materials Research, Part A* 108, no. 4 (2020): 938–946, https://doi.org/10.1002/jbm.a.36871.

33. A Neishabouri, A. Soltani Khaboushan, F. Daghigh, A. M. Kajbafzadeh, and M. Majidi Zolbin, "Decellularization in Tissue Engineering and Regenerative Medicine: Evaluation, Modification, and Application Methods," *Frontiers in Bioengineering and Biotechnology* 10 (2022): 805299, https://doi.org/10.3389/fbioe.2022.805299.

34. M. Trevizani, L. L. Leal, R. J. da Silva Barros, et al., "Effects of Decellularization on Glycosaminoglycans and Collagen Macromolecules in Bovine Bone Extracellular Matrix," *International Journal of Biological Macromolecules* 307 (2025): 41007, https://doi.org/10.1016/j.ijbiomac.2025.141007.

35. F. Y. Zhao, F. Zhao, J. Cheng, et al., "Comparison of Three Different Acidic Solutions in Tendon Decellularized Extracellular Matrix Bio-Ink Fabrication for 3D Cell Printing," *Acta Biomaterialia* 131 (2021): 262–275, https://doi.org/10.1016/j.actbio.2021.06.026.

36. K. Maly, E. Andres Sastre, E. Farrell, A. Meurer, and F. Zaucke, "COMP and TSP-4: Functional Roles in Articular Cartilage and Relevance in Osteoarthritis," *International Journal of Molecular Sciences* 22, no. 5 (2021): 2242, https://doi.org/10.3390/ijms22052242.

37. D. S. Hu and X. L. Shan, "Effects of Different Concentrations of Type-I Collagen Hydrogel on the Growth and Differentiation of Chondrocytes," *Experimental and Therapeutic Medicine* 14, no. 6 (2017): 5411–5416, https://doi.org/10.3892/etm.2017.5202.

38. J. M. Fishman, M. W. Lowdell, L. Urbani, et al., "Immunomodulatory Effect of a Decellularized Skeletal Muscle Scaffold in a Discordant Xenotransplantation Model," *Proceedings of the National Academy of Sciences of the United States of America* 110, no. 35 (2013): 14360–14365, https://doi.org/10.1073/pnas.1213228110.

39. J. R. Fu, E. Wu, G. Li, B. Wang, and C. Zhan, "Anti-PEG Antibodies: Current Situation and Countermeasures," *Nano Today* 55 (2024): 102163, https://doi.org/10.1016/j.nantod.2024.102163.

40. X. Y. Wang, J. Guo, Q. Yu, et al., "Decellularized Matrices for the Treatment of Tissue Defects: From Matrix Origin to Immunological Mechanisms," *Biomolecules & Therapeutics* 32, no. 5 (2024): 509–522, https://doi.org/10.4062/biomolther.2024.050.

41. S. Varghese, N. S. Hwang, A. C. Canver, P. Theprungsirikul, D. W. Lin, and J. Elisseeff, "Chondroitin Sulfate Based Niches for Chondrogenic Differentiation of Mesenchymal Stem Cells," *Matrix Biology* 27, no. 1 (2008): 12–21, https://doi.org/10.1016/j.matbio.2007.07.002.

42. W. H. Yu, W. Yu, Y. Zhu, H. Li, and Y. He, "Injectable Quercetin-Loaded Hydrogel With Cartilage-Protection and Immunomodulatory Properties for Articular Cartilage Repair," *ACS Applied Bio Materials* 3, no. 2 (2020): 761–771, https://doi.org/10.1021/acsabm.9b00673.

43. T. B. Mckay, K. A. Emmitte, C. German, and D. Karamichos, "Quercetin and Related Analogs as Therapeutics to Promote Tissue Repair," *Bioengineering* 10, no. 10 (2023): 1127, https://doi.org/10.3390/bioengineering10101127.

44. C. F. Tsai, G. W. Chen, Y. C. Chen, et al., "Regulatory Effects of Quercetin on M1/M2 Macrophage Polarization and Oxidative/Antioxidative Balance," *Nutrients* 14, no. 1 (2022): 67, https://doi.org/10.3390/nu14010067.

45. K. V. Greco, L. Francis, H. Huang, R. Ploeg, A. R. Boccaccini, and T. Ansari, "Is Quercetin an Alternative Natural Crosslinking Agent to Genipin for Long-Term Dermal Scaffolds Implantation?," *Journal of Tissue Engineering and Regenerative Medicine* 12, no. 3 (2018): e1716–e1724, https://doi.org/10.1002/term.2338.

46. X. Yang, D. Wu, Z. du, R. Li, X. Chen, and X. Li, "Spectroscopy Study on the Interaction of Quercetin With Collagen," *Journal of Agricultural and Food Chemistry* 57, no. 9 (2009): 3431–3435, https://doi.org/10.1021/jf803671s.

47. G. C. Ingavle, A. W. Frei, S. H. Gehrke, and M. S. Detamore, "Incorporation of Aggrecan in Interpenetrating Network Hydrogels to Improve Cellular Performance for Cartilage Tissue Engineering," *Tissue Engineering Part A* 19 (2013): 11–12, https://doi.org/10.1089/ten.tea.2012.0160.

48. J. C. Silva, C. S. M. de Moura, G. Borrecho, et al., "Effects of Glycosaminoglycan Supplementation in the Chondrogenic Differentiation of Bone Marrowand Synovial- Derived Mesenchymal Stem/Stromal Cells on 3D-Extruded Poly (-Caprolactone) Scaffolds," *International Journal of Polymeric Materials and Polymeric Biomaterials* 70, no. 3 (2021): 207–222, https://doi.org/10.1080/00914037.2019.1706511.

49. S. M. Ahmad, H. Hameed, S. A. Al-Hussain, et al., "Chondroitin Sulfate: An Ideal Biomaterial Based Scaffolds for Cartilage Regeneration and Its Therapeutic Potential," *Carbohydrate Polymer Technologies and Applications* 10 (2025): 100742, https://doi.org/10.1016/j.carpta.2025.100742.

50. G. C. Ingavle, N. H. Dormer, S. H. Gehrke, and M. S. Detamore, "Using Chondroitin Sulfate to Improve the Viability and Biosynthesis of Chondrocytes Encapsulated in Interpenetrating Network (IPN) Hydrogels of Agarose and Poly(Ethylene Glycol) Diacrylate," *Journal of Materials Science. Materials in Medicine* 23, no. 1 (2012): 157–170, https://doi.org/10.1007/s10856-011-4499-9.

51. D. O. Freytes, J. Martin, S. S. Velankar, A. S. Lee, and S. F. Badylak, "Preparation and Rheological Characterization of a Gel Form of the Porcine Urinary Bladder Matrix," *Biomaterials* 29, no. 11 (2008): 1630–1637, https://doi.org/10.1016/j.biomaterials.2007.12.014.

52. E. Gossla, A. Bernhardt, R. Tonndorf, D. Aibibu, C. Cherif, and M. Gelinsky, "Anisotropic Chitosan Scaffolds Generated by Electrostatic Flocking Combined With Alginate Hydrogel Support Chondrogenic Differentiation," *International Journal of Molecular Sciences* 22, no. 17 (2021): 9341, https://doi.org/10.3390/ijms22179341.

53. J. Zeng, L. Huang, H. Xiong, et al., "Injectable Decellularized Cartilage Matrix Hydrogel Encapsulating Urine-Derived Stem Cells for Immunomodulatory and Cartilage Defect Regeneration," *npj Regenerative Medicine* 7, no. 75 (2022): 1–12, https://doi.org/10.1038/s41536-022-00269-w.

54. Z. H. Tan, L. Liu, S. Dharmadhikari, et al., "Partial Decellularization Eliminates Immunogenicity in Tracheal Allografts," *Bioengineering & Translational Medicine* 8, no. 5 (2023): e10525, https://doi.org/10.1002/btm2.10525.

55. F. E. Uhl, F. Zhang, R. A. Pouliot, et al., "Functional Role of Glycosaminoglycans in Decellularized Lung Extracellular Matrix," *Acta Biomaterialia* 102 (2020): 231–246, https://doi.org/10.1016/j.actbio.2019.11.029.

56. T. Wang and F. Yang, "A Comparative Study of Chondroitin Sulfate and Heparan Sulfate for Directing Three-Dimensional Chondrogenesis of Mesenchymal Stem Cells," *Stem Cell Research & Therapy* 8, no. 284 (2017): 1–12, https://doi.org/10.1186/s13287-017-0728-6.

57. G. Yazdanpanah, E. Jalilian, X. Shen, et al., "The Effect of Decellularization Protocols on Characterizations of Thermoresponsive and Light-Curable Corneal Extracellular Matrix Hydrogels," *Scientific Reports* 13, no. 1 (2023): 8145, https://doi.org/10.1038/s41598-023-35202-8.

58. P. Guo, N. Jiang, C. Mini, et al., "Decellularized Extracellular Matrix Particle-Based Biomaterials for Cartilage Repair Applications," *Journal of Materials Science and Technology* 160 (2023): 194–203, https://doi.org/10.1016/j.jmst.2023.03.019.

59. G. Singh, S. Satpathi, B. V. Gopala Reddy, et al., "Impact of Various Detergent-Based Immersion and Perfusion Decellularization Strategies on the Novel Caprine Pancreas Derived Extracellular Matrix Scaffold," *Frontiers in Bioengineering and Biotechnology* 11 (2023): 1253804, https://doi.org/10.3389/fbioe.2023.1253804.

60. A. Rafighdoust, N. M. Shahri, and J. Baharara, "Decellularized Kidney in the Presence of Chondroitin Sulfate as a Natural 3D Scaffold for Stem Cells," *Iranian Journal of Basic Medical Sciences* 18, no. 8 (2015): 788–798.

61. Y. F. Fang, Y. Fang, W. Zhou, et al., "Effect of Chemical Modification on Physicochemical and Biological Properties of Chondroitin Sulfate," *Polymer Testing* 115 (2022): 107747, https://doi.org/10.1016/j.polymertesting.2022.107747.

62. S. Dawlee, A. Sugandhi, B. Balakrishnan, D. Labarre, and A. Jayakrishnan, "Oxidized Chondroitin Sulfate-Cross-Linked Gelatin Matrixes: A New Class of Hydrogels," *Biomacromolecules* 6, no. 4 (2005): 2040–2048, https://doi.org/10.1021/bm050013a.

63. H. K. Cheung, T. T. Han, D. M. Marecak, J. F. Watkins, B. G. Amsden, and L. E. Flynn, "Composite Hydrogel Scaffolds Incorporating Decellularized Adipose Tissue for Soft Tissue Engineering With Adipose-Derived Stem Cells," *Biomaterials* 35, no. 6 (2014): 1914–1923, https://doi.org/10.1016/j.biomaterials.2013.11.067.

64. M. A. H. Quijano, N. Sharma, P. Morissette Martin, C. A. Séguin, and L. E. Flynn, "Development of 2-D and 3-D Culture Platforms Derived From Decellularized Nucleus Pulposus," *Frontiers in Bioengineering and Biotechnology* 10 (2022): 937239, https://doi.org/10.3389/fbioe.2022.937239.

65. A. N. Akram and C. Zhang, "Extraction of Collagen-II With Pepsin and Ultrasound Treatment From Chicken Sternal Cartilage; Physicochemical and Functional Properties," *Ultrasonics Sonochemistry* 64 (2020): 105053, https://doi.org/10.1016/j.ultsonch.2020.105053.

66. J. Jin, O. D. Okagu, A. E. G. A. Yagoub, and C. C. Udenigwe, "Effects of Sonication on the in Vitro Digestibility and Structural Properties of Buckwheat Protein Isolates," *Ultrasonics Sonochemistry* 70 (2021): 105348, https://doi.org/10.1016/j.ultsonch.2020.105348.

67. D. Bejleri and M. E. Davis, "Decellularized Extracellular Matrix Materials for Cardiac Repair and Regeneration," *Advanced Healthcare Materials* 8, no. 5 (2019): e1801217, https://doi.org/10.1002/adhm.201801217.

68. A. Almalla, L. Elomaa, L. Bechtella, et al., "Papain-Based Solubilization of Decellularized Extracellular Matrix for the Preparation of Bioactive, Thermosensitive Pregels," *Biomacromolecules* 24, no. 12 (2023): 5620–5637, https://doi.org/10.1021/acs.biomac.3c00602.

69. E. C. Beck, M. Barragan, M. H. Tadros, S. H. Gehrke, and M. S. Detamore, "Approaching the Compressive modulus of Articular Cartilage With a Decellularized Cartilage-Based Hydrogel," *Acta Biomaterialia* 38 (2016): 94–105, https://doi.org/10.1016/j.actbio.2016.04.019.

70. K. Stuart and A. Panitch, "Influence of Chondroitin Sulfate on Collagen Gel Structure and Mechanical Properties at Physiologically Relevant Levels," *Biopolymers* 89, no. 10 (2008): 841–851, https://doi.org/10.1002/bip.21024.

71. R. M. LoPachin and T. Gavin, "Molecular Mechanisms of Aldehyde Toxicity: A Chemical Perspective," *Chemical Research in Toxicology* 27, no. 7 (2014): 1081–1091, https://doi.org/10.1021/tx5001046.

72. J. Fernandez-Perez and M. Ahearne, "The Impact of Decellularization Methods on Extracellular Matrix Derived Hydrogels," *Scientific Reports* 9, no. 1 (2019): 14933, https://doi.org/10.1038/s41598-019-49575-2.

73. C. C. Ai, L. Liu, K. Wong, X. H. Tan, and J. C. H. Goh, "The Effect of Chondroitin Sulfate Concentration and Matrix Stiffness on Chondrogenic Differentiation of Mesenchymal Stem Cells," *Biomaterials Science* 11, no. 13 (2023): 4557–4573, https://doi.org/10.1039/d2bm01980a.

74. B. Bachmann, S. Spitz, B. Schädl, et al., "Stiffness Matters: Fine-Tuned Hydrogel Elasticity Alters Chondrogenic Redifferentiation," *Frontiers in Bioengineering and Biotechnology* 8 (2020): 373, https://doi.org/10.3389/fbioe.2020.00373.

75. J. Lee, J. Y. Lee, B. C. Chae, J. Jang, E. A. Lee, and Y. Son, "Fully Dedifferentiated Chondrocytes Expanded in Specific Mesenchymal Stem Cell Growth Medium With FGF2 Obtains Mesenchymal Stem Cell Phenotype in Vitro but Retains Chondrocyte Phenotype in Vivo," *Cell Transplantation* 26, no. 10 (2017): 1673–1687, https://doi.org/10.1177/0963689717724794.

76. T. Roncada, R. Bonithon, G. Blunn, and M. Roldo, "Soft Substrates Direct Stem Cell Differentiation Into the Chondrogenic Lineage Without the Use of Growth Factors," *Journal of Tissue Engineering* 13 (2022): 20417314221122121, https://doi.org/10.1177/20417314221122121.

77. K. Futrega, P. G. Robey, T. J. Klein, R. W. Crawford, and M. R. Doran, "A Single Day of TGF-1 Exposure Activates Chondrogenic and Hypertrophic Differentiation Pathways in Bone Marrow-Derived Stromal Cells," *Communications Biology* 4, no. 1 (2021): 29, https://doi.org/10.1038/s42003-020-01520-0.

78. M. Kusaczuk, R. Krętowski, M. Naumowicz, A. Stypułkowska, and M. Cechowska-Pasko, "A Preliminary Study of the Effect of Quercetin on Cytotoxicity, Apoptosis, and Stress Responses in Glioblastoma Cell Lines," *International Journal of Molecular Sciences* 23, no. 3 (2022): 1345, https://doi.org/10.3390/ijms23031345.

79. K. W. Ren, Y. H. Li, G. Wu, et al., "Quercetin Nanoparticles Display Antitumor Activity via Proliferation Inhibition and Apoptosis Induction in Liver cancer Cells," *International Journal of Oncology* 50, no. 4 (2017): 1299–1311, https://doi.org/10.3892/ijo.2017.3886.

80. E. J. Sohn, J. M. Kim, S. H. Kang, et al., "Restoring Effects of Natural Anti-Oxidant Quercetin on Cellular Senescent Human Dermal Fibroblasts," *American Journal of Chinese Medicine* 46, no. 4 (2018): 853–873, https://doi.org/10.1142/S0192415X18500453.

81. M. Zawani, M. Maarof, Y. Tabata, A. Motta, and M. B. Fauzi, "Quercetin-Embedded Gelastin Injectable Hydrogel as Provisional Biotemplate for Future Cutaneous Application: Optimization and in Vitro Evaluation," *Gels* 8, no. 10 (2022): 18, https://doi.org/10.3390/gels8100623.

Supporting Information

Additional supporting information can be found online in the Supporting Information section. **Figure S1:** FTIR of aldehyde modified chondroitin sulphate. FTIR spectrum for both chondroitin sulphate (CS) and aldehyde modified chondroitin sulphate (mCS). Aldehyde peak was observed at 1738 cm^{-1}. **Figure S2:** Rheological analysis spectra for decellularised cartilage-based hydrogels and with modified/non-modified chondroitin sulphate functionalised gels. (A, D) G', (B, E) G'', (C, F) G*. (A–C) Frequency analysis from 0.1 to 10 Hz with 1% strain. (D–F) Strain amplitude of 0.1% to 100% with 1 Hz frequency. **Figure S3:** Rheological analysis spectra for dECM, aldehyde modified chondroitin sulphate functionalised hydrogels and quercetin incorporated functionalised hydrogels. (A, D) G', (B, E) G'', (C, F) G*. (A–C) Frequency analysis from 0.1 to 10 Hz with 1% strain. (D–F) Strain amplitude of 0.1% to 100% with 1 Hz frequency. **Figure S4:** in vitro gene expression of extracellular matrix components. mRNA expression level of (1-6A) Collagen type 2 (COL2A1), (1-6B) Aggrecan (ACAN), (1-6C) Cartilage oligomeric matrix protein (COMP), (1-6D) Collagen type 1 (COL1A1), (1-6E) Collagen type 10 (COL10A1), (1-6F) Alkaline phosphate (ALPL) by quantitative real-time PCR of cell seeded gels after 21 days of in vitro culture. (1–3) Hydrogels observed included the dECM hydrogel along with non-modified (CS) and modified (mCS) functionalised gels with

concentrations of 0.2 mg/mL and 0.4 mg/mL. (4–6) Hydrogels observed included the dECM hydrogel along with 0.4 mg/mL mCS with this hydrogel being then incorporated with quercetin at concentrations of 0.15 mg/mL and 0.3 mg/mL. Fold change (ΔΔCT) to control samples, being the dECM hydrogel. Error bars represent upper and lower limits ($n = 2$). **Figure S5:** In vitro gene expression of extracellular matrix components. mRNA expression level of (1-3A) Collagen type 2 (COL2A1), (1-3B) Aggrecan (ACAN), (1-3C) Cartilage oligomeric matrix protein (COMP), (1-3D) Collagen type 1 (COL1A1), (1-3E) Collagen type 10 (COL10A1), (1-3F) Alkaline phosphate (ALPL) by quantitative real-time PCR of cell seeded hydrogels after 21 days of in vitro culture. Hydrogels observed included the dECM hydrogel along with 0.4 mg/mL mCS hydrogel with this being then incorporated with quercetin at concentrations of 0.15 mg/mL and 0.3 mg/mL. Fold change (ΔΔCT) to control samples, being the dECM hydrogel. Error bars represent upper and lower limits ($n = 3$). Depending on the normal distribution, the statistical analysis undertaken either with (1) One-Way ANOVA test followed by Tukey's multi-comparison test (2) Kruskal-Wallis test followed by Tukey's multi-comparison test $p < 0.05$ (*), $p < 0.01$ (**). **Table S1:** Statistical analysis of G', G'' and G* over strain amplitude for supplementary Figure S3. The statistical analysis undertaken with RM two-way ANOVA with the Geisser–Greenhouse correction followed by Tukey's multiple comparisons test $p < 0.05$ (*), $p < 0.01$ (**). **Table S2:**. Statistical analysis of G', G'' and G* over Frequency for supplementary Figure S3. The statistical analysis undertaken with RM two-way ANOVA with the Geisser–Greenhouse correction followed by Tukey's multiple comparisons test $p < 0.05$ (*).